Journal of Archaeological Method and Theory (2020) 27:930–970
https://doi.org/10.1007/s10816-020-09448-9

Red Earth, Green Glass, and Compositional Data: A New Procedure for Solid-State Elemental Characterization, Source Discrimination, and Provenience Analysis of Ochres

Andrew M. Zipkin, et al. *[full author details at the end of the article]*

Published online: 22 February 2020

Abstract

Ochres are a diverse category of naturally occurring iron-enriched earths and rocks, as well as iron oxide minerals, that derive their color from iron-containing chromophores and are suitable for use as pigments. Over the last two decades, provenience studies of archaeological ochres have grown from a rarity largely of interest only to specialists to an accepted and expected part of the archaeological science panoply. The most effective approach to distinguishing among sources of ochre and assigning archaeological pigments to their origin is multi-elemental characterization or "elemental fingerprinting." In this study, we coupled a sample preparation method not previously used in ochre archaeometry with elemental fingerprinting by Laser Ablation-Inductively Coupled Plasma-Mass Spectrometry (LA-ICP-MS) and Electron Probe MicroAnalysis (EPMA). We present a procedure for lithium borate (LiBo) fusion of samples for solid-state analysis, optimized for use with ochres, and designed for the budget and laboratory equipment constraints faced by many professional and student archaeologists. This method development research is part of the broader project "OLKARIA: Ochre Landscapes of Kenya – Anthropological Research and Iron-oxide Archaeometry," which seeks in part to characterize the elemental composition of all known geologic ochre sources in the Kenya Rift Valley. Using a subset of project OLKARIA samples prepared by LiBo fusion and measured with LA-ICP-MS and EPMA, we successfully distinguished among six geologic ochre sources and a sample of commercially available iron oxide pigment. Our ability to uphold the Provenience Postulate for this data set compared favorably with source discrimination analyses done using data from Neutron Activation Analysis (NAA) of whole ochre for the same samples. LiBo fusion presents potential solutions to some criticisms of solid-state analysis of ochre using beam techniques, including issues arising from mineralogical heterogeneity, variable surface topography, the presence of free and chemically bound water, and the lack of matrix-matched standard reference materials. We also address the challenges of applying compositional data analysis best practices to ochre with an emphasis on the issues

Electronic supplementary material The online version of this article (https://doi.org/10.1007/s10816-020-09448-9) contains supplementary material, which is available to authorized users.

of rounded zero replacement and multivariate normality and highlight the work that remains to be done in this area.

Keywords Iron oxide · Lithium borate fusion · LA-ICP-MS · EPMA · NAA · Provenance · Provenience · Censored data · Rounded zero replacement

Introduction

Ochres are a diverse category of naturally occurring iron-enriched earths and rocks, as well as iron oxide minerals, that derive their color from iron-containing chromophores and are suitable for use as pigments (Cornell and Schwertmann 2003; Froment *et al.* 2008; Popelka-Filcoff *et al.* 2008). Pigments in general and ochres in particular have long been acknowledged as a significant part of the material culture record of the last 300,000 years (Farnsworth 1951; Dart 1968; Wreschner *et al.* 1980; Brooks *et al.* 2018). In prehistoric archaeology, ochres are particularly notable for their use as a vehicle for symbolism that is both geographically widespread and durable enough to be visible in the material culture record. The first compositional studies of ancient pigments were published in the early nineteenth century and focused on painted art objects and excavated caches of prepared colors from Classical Greece and Rome (Chaptal 1809; Davy 1815). They are among the first works of archaeological chemistry. A few earlier examples include Dizé's (1790) gravimetric analysis of copper alloy coins, Pearson's (1796) experiments on metallic arms and utensils recovered from an English river, and Klaproth's (1798) much cited work on Roman and Greek coins and glass. Despite the early origins of pigment analysis in archaeology and art history, the study of ochre from a geochemical sourcing perspective has developed into distinct sub-specialty within the archaeological sciences only during the last two decades (Chalmin and Huntley 2017). This manuscript serves multiple purposes; first and foremost, we present a combined sample preparation, instrumental analysis, and data processing procedure for elemental characterization that has not previously been used in ochre archaeometry. We additionally address complementary issues, including situating sourcing studies within archaeological theory, and best practices for instrumental method selection and compositional data analysis.

Provenance and provenience studies in archaeology have flowered since the development of instrumental methods for compositional analysis following the Second World War, particularly Neutron Activation Analysis (NAA; Pollard *et al.* 2007). In a previous work (Zipkin *et al.* 2017), we addressed the distinction between provenance and provenience, building on Weigand *et al.* (1977), Neff (2000), Wilson and Pollard (2001), Price and Burton (2011), Joyce (2012, 2013), and Pollard *et al.* (2014). The two terms have been used inconsistently in archaeometry since at least the early 2000s. It is tempting to blame this in part on the revision of the original Weigand *et al.* "Provenience Postulate" (1977) to the "Provenance Postulate" of Neff (2000). Neff stated that "Weigand and his colleagues named this the 'Provenience Postulate'; I will refer to it as the 'provenance postulate' in order to avoid confusion arising from the fact that the term 'provenience' is also used as a synonym for archaeological context." However, confusion over the two terms is far older than Neff (2000) or Weigand *et al.* (1977). Joyce (2012) traces distinct uses of provenience and provenance to the late nineteenth

century and complaints over their perceived misuse to the early twentieth. In their 2011 book *An Introduction to Archaeological Chemistry*, Price and Burton titled a chapter "Provenience and Provenance" and went on to say that the two terms are variably synonymous and distinct depending on the academic field (*e.g.*, art history, archaeology, geology/sedimentology) and national professional tradition.

Following Joyce (2012), we advocate for a clearer conceptual distinction and use of these terms and expand our earlier discussion (Zipkin *et al.* 2017) here to address their relevance for anthropological archaeology, materiality, and bioarchaeology. We define provenience narrowly as a spatial location. It includes archaeological provenience (coordinates and context within an archaeological site) and source provenience (geographic origin of raw material). Source provenience may be a specific geologic deposit of the raw material itself, such as a single obsidian flow with mapped boundaries, or a broader classification like all obsidian flows derived from the same magma chamber or a limestone formation that hosts chert nodules. Frahm (2014) provides a valuable discussion of what constitutes an obsidian source and what "sourcing" an artifact means. For materials that may be synthetic composites from two or more sources and may include recycled ingredients, such as smelted metals, glasses, and ceramics, source provenience is the production site (Pollard and Heron 2008; Zhu *et al.* 2012). Biogenic materials like enamel and bone may be sourced to the region from which an organism acquired nutrition based on elemental and isotopic signatures transmitted from diet to hard tissue.

Provenance is a broader behavioral concept that begins and ends with spatial provenience. It encompasses all natural and cultural processes that contribute to object biographies (Gosden and Marshall 1999), including but not limited to raw material extraction, manufacture, transport, exchange, use, discard, deposition, taphonomic alteration, excavation, and curation history. These processes and events can be considered components of the life histories of any objects with which humans interact. Building on an anecdote cited by Price and Burton (2011), we succinctly explain source provenience as analogous to the birthplace and archaeological provenience to the final resting place recorded by a tombstone, while provenance is analogous to an obituary in *The New York Times* – a narrative of an individual's biography from birth to death.

The life history/biography concept of provenance can also be applied to archaeological sites, structures, rock art sites, and other places on the landscape where human activities occur in the same place over time. To paraphrase Geertz's (1973) memorable formulation, landscape is a story people tell themselves about themselves. For example, a cemetery is not a static feature of the landscape: although populated by the dead, it is an ongoing product of the living. It acquires its own biography as new burials and markers are added over time, rituals are performed, offerings are left by visitors, and sites are abandoned or repurposed. The biography of rock art and other sites with stratified deposits also has important implications for understanding how humans claim and use landscape features. Geochemical sourcing of rock art pigments, especially in cases of overpainting and reuse of a space, has the potential to shed light on temporal patterns of pigment source exploitation, changing uses of the same site, and even competing territorial claims to the same places by different groups (*e.g.*, Smith *et al.* 1998). The provenance/life history concept can also be applied to human and nonhuman animal skeletons and other tissues. The genetic, elemental, and isotopic

composition of tissues preserves records of ancestry, diet, and environment at different points during development. Skeletal geochemistry also contributes to reconstructions of seasonal mobility and longer-term residential histories and thus to the osteobiography and provenance of individuals (Williamson and Pfeiffer 2003; Gregoricka 2014).

In this study, we focus on analytical chemistry methods that can be used to determine the geologic provenience of ochre as a stepping-stone towards the reconstruction of provenance. Determination of provenience permits, at a minimum, estimation of distance from source to site. The nature of how ochre was transported, whether via direct procurement, down the line exchange, or systematic bulk commodity transport (Renfrew 1977) requires inferences and tests of alternative hypotheses. Ochre pigments may have had a variety of utilitarian functions as well as important roles in the symbolic and social lives of past societies (Hovers *et al.* 2003; Trinkaus and Buzhilova 2018). Some documented and proposed utilitarian roles include mosquito repellent (Rifkin 2015), sunscreen (Rifkin *et al.* 2015), hide preservative (Audouin and Plisson 1982), and ingredient in composite tool hafting adhesives (Brandt and Weedman 2002; Wadley 2005; Zipkin *et al.* 2014). Examples of symbolic uses of ochre include personal adornment/cosmetics (Thackeray *et al.* 1983; Saitoti 1993; Nakamura 2005), engraving substrate (Mackay and Welz 2008; Henshilwood *et al.* 2009), and rock art pigment (Chamberlain 2006; Arocena *et al.* 2008; Scadding *et al.* 2015). Distinguishing among such applications, and the symbolic, functional, or dual roles of ochres, in the archaeological record remains a challenge. Accurate and reproducible provenience studies of ochres can thus contribute to anthropological archaeology goals such as identifying utilitarian versus symbolically mediated resource extraction and reconstruction of mobility, exchange, trade, social networks, and provisioning landscapes.

Since 2010, we have worked to develop a reference data set of geologic ochre source elemental "fingerprints" for the Kenya Rift Valley and adjacent regions through the project "OLKARIA: Ochre Landscapes of Kenya – Anthropological Research and Iron-oxide Archaeometry." Ultimately this collection of chemical and spatial data from multiple field seasons and publications will be made publicly and permanently available in one location through the Digital Archaeological Record (tDAR) for new interpretations by any interested researcher. Reference specimens from all ochre sources sampled from 2010 through present have been stored at the National Museums of Kenya (NMK), Nairobi, and at the University of Illinois at Urbana-Champaign, and can be accessed for future analysis through the NMK or by contacting co-author Stanley Ambrose. This project will facilitate new sourcing studies of archaeological and ethnographic ochre without the need to conduct expensive, time-consuming, and redundant source surveys and sampling. Figure 1 shows the sources discussed in this study only; over 40 additional sources have been identified and sampled at this time.

Analytical chemistry method development has also been a major feature of this project. Our goal in this area has been the development of a standard operating procedure that is within the technological and financial reach of most archaeologists and facilitates accurate and precise concentration measurements for much of the periodic table. We present a sample preparation method, lithium borate (LiBo) fusion, that may be used to vitrify ochre into a homogeneous glass suitable for elemental composition analysis. Using a selection of Kenyan ochres from our broader source characterization project, we demonstrate that lithium borate fusion followed by

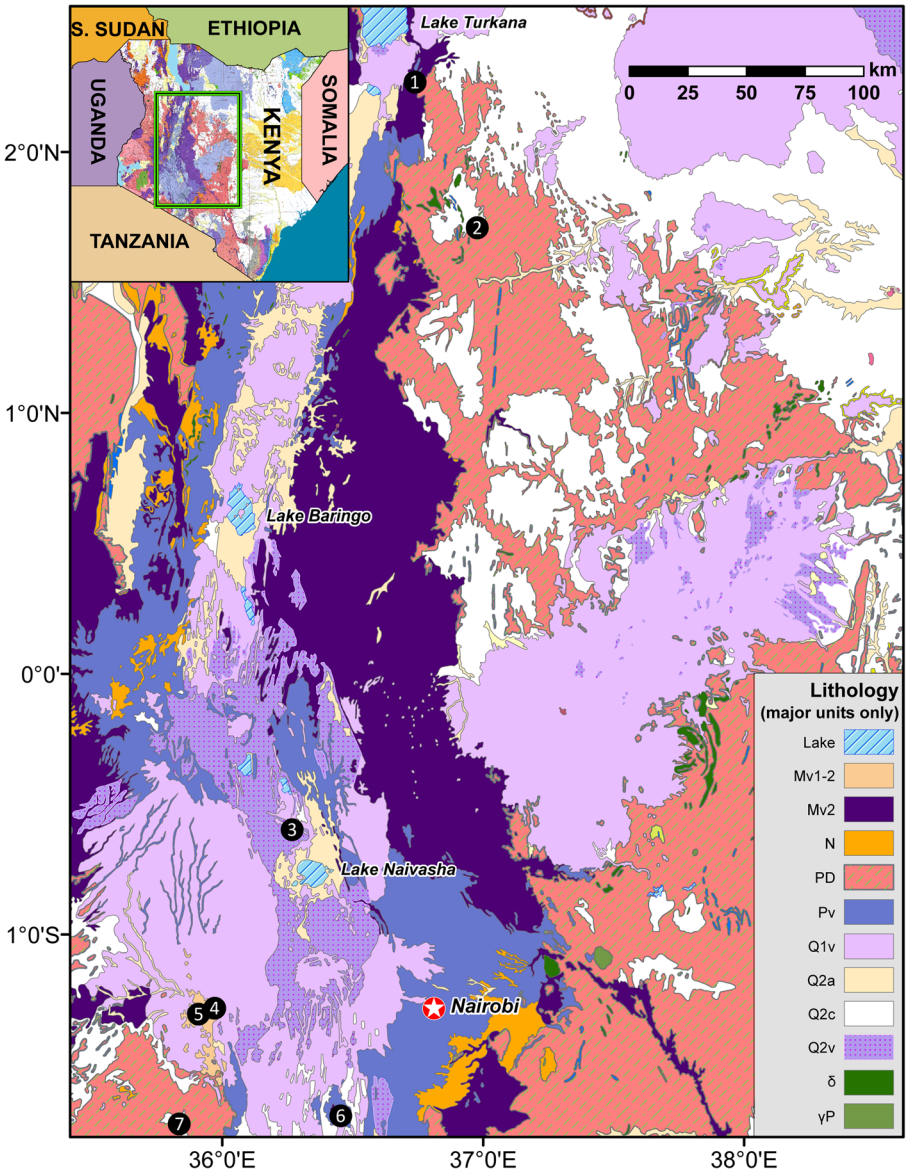

Fig. 1 Map of Kenyan ochre acquisition locations (black numbered circles) for samples analyzed in this study. 1, Karia Ejuk; 2, Ngurunit Market; 3, Kitumbo/Ewaji Naado; 4, Emurua Dikir; 5, Indoinyo Ereko; 6, Olorgesailie; 7, Napolosa. Note that Ngurunit is not a geological source (see text). Lithology is derived from the 1987 Geological Map of Kenya, Ministry of Energy and Regional Development of Kenya. This map was digitized by Orr and Associates (Australia) and the ASU Library Map and Geospatial Hub. Lithology of mapped units (unit codes from original map): *Mv1–2* Upper Oligocene-Upper Miocene phonolites, trachytes, and olivine basalts; *Mv2* Upper Miocene phonolites, trachytes, and olivine basalts; *N* Neogene undifferentiated sediments interbedded in volcanics; *PD* Precambrian D – Mozambique belt, quartzites, mica schists, biotite and hornblende gneiss, granitoid gneiss, amphibolites, migmatites, and syntectonic granites; *Pv* Pliocene trachytes, phonolites, and basalts; *Q1v* Pleistocene trachytes, basalts, and pyroclastics; *Q2a* Holocene alluvium, dunes, and beaches; *Q2c* Holocene colluvial deposits, pebble sheets and red soils, and old surface (Garissa); *Q2v* Holocene basalt flows, pyroclastics, and volcanic soils; *δ* Precambrian to Tertiary basic rocks; *γP* undifferentiated Precambrian

Electron Probe MicroAnalysis (EPMA) and Laser Ablation-Inductively Coupled Plasma-Mass Spectrometry (LA-ICP-MS) facilitates collection of major, minor, and trace element concentrations and permits discrimination among ochre sources with high confidence. Analysis of LiBo fused glass using beam techniques is minimally destructive and permits multiple replicate analyses of the same prepared sample. This makes it easier to evaluate instrumental and methodological accuracy and precision and can improve the power of multivariate statistical procedures used to test the Provenience Postulate for source discrimination. The Provenience Postulate is satisfied if variation in chemical composition within sources is less than the differences among sources (Weigand *et al.* 1977). The long-term stability of LiBo fused glass will facilitate evaluation of reproducibility of measurements among laboratories and meta-analyses of results from multiple projects. The LiBo fused ochre samples and quality control standards discussed in this study are suitable for analysis using techniques like Scanning Electron Microscopy-Energy Dispersive Spectroscopy (SEM-EDS), X-Ray Fluorescence (XRF), EPMA, and LA-ICP-MS and are available from author Andrew Zipkin to any researchers who wish to evaluate the reproducibility of the results presented here.

Selection of Instrumental Methods for Ochre Elemental Composition Analysis

A remarkably diverse range of techniques has been used to characterize the chemical composition of ochre (Zipkin *et al.* 2015). The methods presented in this report, and those from a selection of previous studies described in Table 1 below, focus on the analysis of discrete pieces of lithified pigment and bulk unlithified ochre, including iron oxide-containing clays and soils. This contrasts with surficial adhering layers of ochre such as rock art paint, residues on artifacts, and pottery slips (Russ *et al.* 2012; d'Errico *et al.* 2016). Pigments applied to or deposited on surfaces may have been deliberately or inadvertently mixed with other materials such as adhesives, dilutants, or multiple pigment types. They may also be susceptible to contamination from the surfaces that they adhere to, or the characterization method may analyze the pigment layer together with its underlying substrate and overlying accretions (Huntley 2012). Surficial pigments require specialized sample collection, chemical analysis, and data interpretation methods (*e.g.*, Chalmin and Huntley 2017) outside the scope of this study, though the methods presented here may be adaptable for use with pigment residues after further development.

We suggest that the work presented here can serve as the basis for a standardized preparation method that will produce homogeneous samples from heterogeneous materials, which will then be suitable for several kinds of instrumental analyses. For compositional analysis of ochres, we advocate using three criteria to narrow the range of instrumental methods under consideration: (1) which variables can be measured and with what precision, (2) the minimum sample size (mass or dimensions) required for analysis and the maximum permitted, and (3) whether the method is damaging to the original specimen, destructive to the analyzed sample, or both. A related consideration is whether multiple methods are complementary or redundant and whether those methods require separate sub-samples from a specimen or permit analysis of a prepared sample by more than one instrumental method. Table 1 presents a limited selection of examples from ochre archaeometry studies of the last decade that span most of the range of these criteria.

Table 1 Examples of methods used for elemental analysis of bulk ochre, excluding studies that only analyzed ochre-based paints, pottery slips, and residues

Instrumental methods {reference #}+	Summary sample preparation methods	Reported mass or dimensions of analyzed specimens	Elements reported for ochres (excludes elements only measured in standard reference materials)*
Comparator Neutron Activation Analysis (NAA) {1}	Low temperature drying, then homogenized by mortar and pestle	1 g	Al, Ca, Fe, Na, Ti, V, Mn, K, Cl, Cr, Sc, Co, Zn, As, Sb, Ba, Cs, Hf, Ta, La, Ce, Nd, Sm, Eu, Tb, Dy, Yb, Lu, Th (quantitative)
Comparator NAA {2}	Low temperature drying, then homogenized by mortar and pestle	Short irradiation samples: 75–85 mg; long irradiation samples: 95–105 mg	Al, As, Ba, Ca, Ce, Co, Cr, Cs, Dy, Eu, Fe, Hf, K, La, Lu, Mn, Na, Nd, Ni, Rb, Sb, Sc, Sm, Sr, Ta, Ti, Tb, Th, U, V, Yb, Zn, Zr (quantitative)
k0-NAA (standard-less) and NAA (traditional relative comparator as above) {3}	Low temperature drying, and a mixer mill or mortar and pestle to homogenize samples	120 mg: assumed to be comparable for both NAA methods	k0-NAA and NAA: Al, As, Ba, Ca, Ce, Co, Cr, Cs, Dy, Eu, Fe, Hf, K, La, Lu, Mn, Na, Nd, Ni, Rb, Sb, Sc, Sm, Sr, Ta, Tb, Th, Ti, U, V, Yb, Zn, Zr (quantitative) k0-NAA only: Ag, Ar, Au, Br, Cd, Cl, Cu, Er, Ga, Gd, Ge, Hg, Ho, I, In, Ir, Mg, Mo, Nb, Os, Pd, Pr, Pt, Re, Rh, Ru, S, Se, Sn, Te, Tm, W, Y (quantitative)
Laser Ablation--Inductively Coupled Plasma-Mass Spectrometry (LA-ICP-MS) {4}	"Minute" samples of solid ochre removed from larger pieces	Not stated; 3 replicate ablations done per piece using scan lines with 100-μm spot size	Ca, Sc, Ti, V, Cr, Mn, Fe, Co, Ni, Cu, Zn, Ga, Ge, As, Se, Rb, Sr, Y, Zr, Nb, Mo, Pd, Ag, Cd, In, Sn, Sb, Te, Cs, Ba, La, Ce, Pr, Nd, Sm, Eu, Gd, Tb, Dy, Ho, Er, Tm, Yb, Lu, Hf, Ta, W, Au, Hg, Tl, Pb, Bi, Th, U (qualitative, according to authors) (in cps-counts per second, not ppm (parts per million))
LA-ICP-MS and Electron Probe MicroA nalysis (EPMA) {5}	Mortar and pestle homogenized, mixed with epoxy, and cured. ~ 1-mm^2 chip mounted for analysis	1 g: same chip used for LA-ICP-MS and EPMA; minimum mass is 50–100 mg whole ochre	LA-ICP-MS: Mg, Si, P, Ca, Sc, Ti, V, Cr, Mn, Zn, As, Sr, Y, Zr, Nb, Sn, Ba, La, Ce, Pr, Nd, Sm, Eu, Gd, Tb, Dy, Ho, Er, Tm, Yb, Lu, Hf, Ta, Pb, Th, U (quantitative); EPMA: Fe (used as internal standard for LA-ICP-MS data reduction per Longerich *et al.* 1996)
Inductively Coupled Plasma-Optical Emission Spectrometry (ICP-OES) and ICP-MS {6}	Homogenized to powder, fused with LiBo, molten fusion dissolved in nitric acid	200 mg: assumed that both methods were done on the same sample solution	ICP-OES: Na, Mg, Al, Si, P, K, Ca, Ti, Mn, Fe (quantitative); ICP-MS: V, Cr, Co, Ga, As, Rb, Sr, Y, Zr, Nb, Sb, Ba, Ta, Pb, U (quantitative)

Table 1 (continued)

Instrumental methods {reference #}+	Summary sample preparation methods	Reported mass or dimensions of analyzed specimens	Elements reported for ochres (excludes elements only measured in standard reference materials)*
ICP-OES and portable X-Ray Fluorescence (pXRF) {7}	ICP-OES: microwave assisted acid digestion for solution analysis; pXRF: none, nondestructive	ICP-OES: 250 mg; pXRF: minimum mass 0.05 g (2-mm minimum thickness)	ICP-OES: Ti, V, Cr, Mn, Co, Cu, Sr, Zr (quantitative); pXRF: Al, Si, K, Ca, Fe, As, (qualitative-presence/-absence); Ti, V, Cr, Mn, Cu, Sr, Zr (qualitative and quantitative)
Particle Induced X-Ray Emission (PIXE) {8}	None, nondestructive	Specimen dimensions not stated; 1-mm^2 area analyzed	Mg, Al, Si, P, K, Ca, Ti, V, Mn, Fe, Ni, Zn, As, Y, Zr (quantitative)
Scanning Electron Microscopy-Energy Dispersive Spectroscopy (SEM-EDS) {9}	Low temperature grinding, then homogenized using a mortar and pestle	Individual particles (< 10 μm)	Mg, Al, Si, S, Cl, K, Ca, Ti, V, Cr, Mn, Fe (quantitative)

Some studies above also used complementary techniques to determine mineralogy; parameters for those methods are not described. *As used here, "quantitative" refers to measurements that yield reference standard-calibrated concentrations (*e.g.,* 107 ppm), "semi-quantitative" describes measurements that either yield ranges (*e.g.,* 10–20 ppm) or relative proportions (*e.g.,* twice as much Fe as Si), and "qualitative" results only encompass presence, absence, or inconclusive.

+ 1. MacDonald *et al.* 2013; 2. The present study; 3. Popelka-Filcoff *et al.* 2012; 4. Scadding *et al.* 2015; 5. Zipkin *et al.* 2017; 6. Dayet *et al.* 2016; 7. Moyo *et al.* 2016; 8. Mathis *et al.* 2014; 9. Sajó *et al.* 2015

Any project that uses chemical analysis of ochres should have already identified a compelling anthropological, geological, or method development research question prior to selection of instrumental techniques. In addition to being good practice generally, this also helps prevent "methodological overkill" – the inappropriate use of excessively destructive, expensive, difficult, or time-consuming techniques – when an alternative can answer the question with comparable effectiveness. A research question with clearly defined operational parameters will guide consideration of the first factor: which variables must be measured to test a hypothesis? For example, if a research question about archaeological pigments only requires ruling out potential geologic sources of known composition, then a non-destructive method such as calibrated quantitative XRF on bulk samples to measure known elements of interest may be preferable to more labor-intensive techniques. A study that seeks to develop a reference data set for multiple previously uncharacterized ochre sources and to assign archaeological artifacts to specific sources at the local or regional scale, or both, may require a more comprehensive approach that measures dozens of major, minor, and trace elements to determine which are relevant for source discrimination. LiBo fusion of ochre and quantitative multi-elemental characterization is applicable to the latter scenario. By presenting this procedure in detail sufficient for use, refinement, and validation by other researchers, we believe that it can become a first-line method for the construction of ochre geochemical reference data sets.

Once the relevant variables have been identified, along with techniques capable of adequately measuring them, the remaining two criteria can be applied to narrow the options further. Analysis of geological ochre samples permits the use of bulk methods such as NAA, or LiBo fusion of comparable sample masses, because availability of material is usually not a limiting factor. Options for compositional analysis of archaeological materials may be limited by specimens that are too small for a selected method or that may not be sampled destructively. Alternatively, large specimens may be prohibitive for a method like *in situ* LA-ICP-MS which, while technically minimally destructive, is often limited by the size of the ablation cell to specimens smaller than a few centimeters and thus requires destructive sub-sampling of larger pieces. Before ruling out instrumental methods based on their common sample size parameters as described in the literature, it is worth consulting experts to determine whether samples may be scaled down or instrumentation modified without sacrificing the quality of results. Archaeological artifacts are a culturally significant non-renewable resource and have associated ethical and legal stipulations that present special challenges for the application of destructive analytic techniques (Mills *et al.* 2008; Prendergast and Sawchuk 2018). If a destructive technique satisfies the first two criteria, then the third consideration is how much of an archaeological artifact will be removed and whether that sample may be reanalyzed later or is consumed entirely. It is this final condition that in part led us to develop the lithium borate fusion approach for use with ochres. Any morphological (*e.g.*, SEM), molecular/structural (*e.g.*, X-ray Diffraction, Raman, Fourier Transform Infrared Spectroscopy), or magnetic (*e.g.*, Mössbauer) analyses must be conducted on bulk ochre prior to fusion to glass. However, once a sample has been prepared by lithium borate fusion, major and minor elements may be measured by EPMA or XRF separately from trace element analysis by LA-ICP-MS using the same fused samples. If sources can be discriminated and artifacts assigned to them based on major and minor element variables, no further analyses are required, or LA-ICP-MS may proceed if needed to yield a complementary data set without requiring additional destructive sampling.

Methods

Borate fusion was introduced by Claisse (1957) for preparation of XRF samples as an alternative to and improvement on analysis of pressed powders or polished solids. *Physics and Chemistry of Borate Fusion* (Claisse and Blanchette 2004) and *Fusion and fluxes* (Claisse 2003) are particularly valuable short works for understanding the principles of fusion and for helping researchers adapt the methods presented here. Individual researchers and industrial reagent manufacturers have developed customized blends of lithium metaborate ($LiBO_2$, LiM), lithium tetraborate ($Li_2B_4O_7$, LiT), non-wetting agents (NWAs, *e.g.*, lithium bromide, LiBr), and oxidizers for use in fusing materials of diverse compositions. Although LA-ICP-MS was invented in the 1980s (Gray 1985; Sylvester and Jackson 2016), analysis of geological samples processed by LiBo fusion with this method only rose to prominence in works such as Nesbitt *et al.* (1997), Günther *et al.* (2001), and Eggins (2003). In archaeological chemistry, examples of lithium borate fusion used to create beads for solid-state analysis include Falcone *et al.* (2002), Nakayama *et al.* (2012), and Ichikawa and Nakamura (2014).

Notably, all of these studies used XRF. A study of reminiscent of our own, Scheid *et al.* (2009), compared LA-ICP-MS and XRF measurements of LiBo fused brick to NAA measurements of whole brick for forensic chemistry applications. We have not located any published examples of LA-ICP-MS of fused beads made from ochre.

In this study, we report the results of LA-ICP-MS and EPMA on 36 LiBo fused ochre samples from seven sources in Kenya, collected during our broader source sampling program: six geologic deposits and a single sample of ochre purchased in a village market in northern Kenya (Fig. 1, Supplementary Table 1). Samples were collected during fieldwork conducted in 2010, 2012, and 2015 and represent a diverse cross-section of materials that can be considered ochre. Supplementary Table 1 identifies each ochre source by type and collection context; ochres analyzed here range from unlithified clay-rich weathering products of volcanic rocks to pisolitic iron ore to commercially available iron oxide pigment. All bulk ochre samples collected during fieldwork were air-dried and split into reference sub-samples accessioned at the Nairobi National Museum, Kenya, and analysis sub-samples exported to the USA before any further processing steps were done. The analysis sub-samples were oven-dried at 50 °C for at least 48 hours in aluminum foil drying dishes (Fig. 2a) and then manually ground to silt-size and smaller particles (< 0.0625 mm) and homogenized using an agate mortar and pestle. Each mortar and pestle pair was cleaned between samples using the following steps to prevent cross-contamination: rinsing with distilled water, grinding with clean quartz sand, rinsing with 6 molar hydrochloric acid, and rinsing again with distilled water. After grinding, each ochre sample was split into one fraction to be analyzed by NAA at the University of Missouri Research Reactor (MURR) Archaeometry Laboratory and a second fraction to be processed using LiBo fusion followed by EPMA and LA-ICP-MS.

NAA Methods

Bulk ground ochre samples were submitted to MURR for NAA on an external laboratory fee-for-service basis; all subsequent sample processing, instrumental analysis, and data reduction were performed by MURR Archaeometry Laboratory staff. Our goal was to obtain results that would permit a functional comparison of whether elemental data measured by LiBo LA-ICP-MS were as effective as NAA concentrations at upholding the Provenience Postulate through multivariate statistical discrimination of sources. NAA is a well-established and widely applied method for quantifying elemental concentrations in ochres and has been successfully used for geologic source discrimination in multiple published studies (*e.g.*, Kiehn *et al.* 2007; Popelka-Filcoff *et al.* 2007, 2008; Eiselt *et al.* 2011; Kingery-Schwartz *et al.* 2013; Velliky *et al.* 2019). The practice of discriminating among ochre sources using NAA-derived elemental data was originally developed at MURR for a pilot study by Ellis *et al.* (1997) and further refined there by Popelka-Filcoff for her doctoral dissertation (2006). All the above cited publications built on the expertise developed during those two pioneering projects and used NAA data collected at MURR. Additionally, ochre samples previously submitted by the lead author to MURR for NAA generated results effective for source discrimination in Malawi (Zipkin *et al.* 2015). An important caveat is that NAA of ochre at MURR uses analytical parameters optimized for clays and ceramics (Kiehn *et al.* 2007; *pers. comm.* Glascock, Group Leader, Archaeometry Laboratory, MURR).

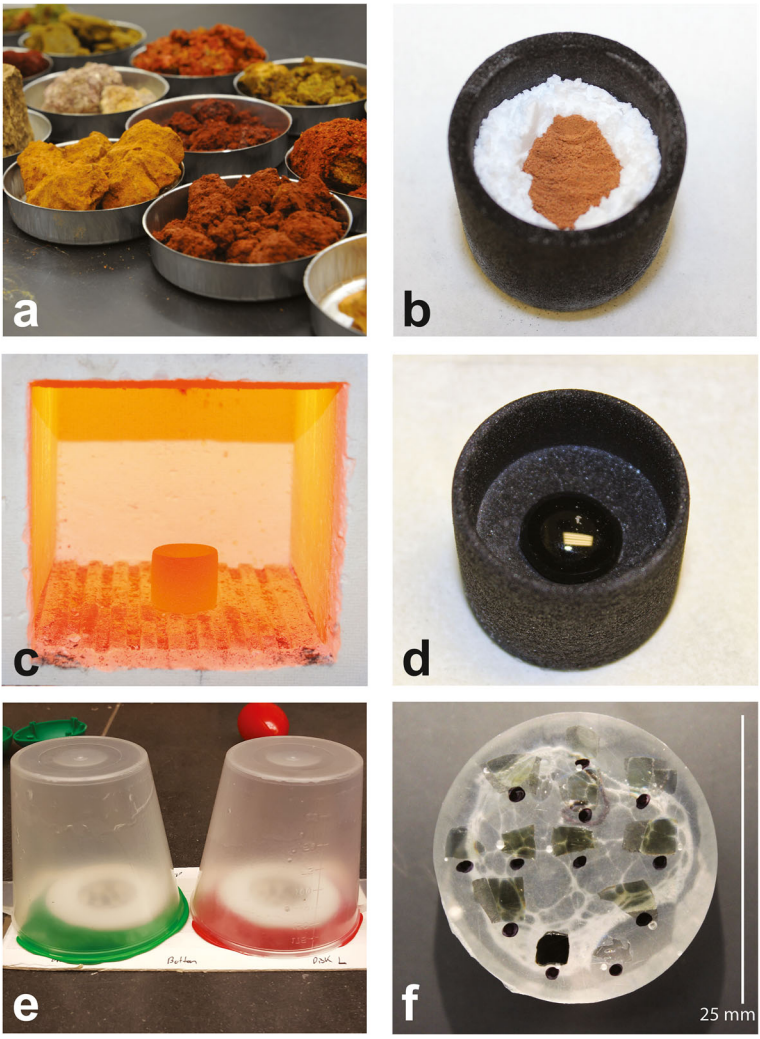

Fig. 2 Composite of processing steps for lithium borate fusion of ochre for solid-state analysis. **a.** Bulk ochre in aluminum trays for oven drying; these are geologic source samples in their collected form prior to grinding in an agate mortar and pestle and subsampling for LiBo fusion and NAA. **b.** Ground ochre nestled in a divot in the lithium borate flux blend in a graphite crucible; it is critical that the ochre sample does not directly contact the crucible. **c.** Furnace with graphite crucible during fusion at 1050 degrees C. **d.** Fused bead in graphite crucible after cooling. **e.** Embedding samples in epoxy – cardboard sheet covered in double-sided tape, PTFE ring mold with 25 mm internal diameter on tape, sealed around perimeter with Silly Putty™, fused bead shards secured on tape inside mold and epoxy poured over until submerged completely, and mold covered with beaker so that hardener does not evaporate before epoxy cures. **f.** Cured epoxy disk after polishing. Black dots were drawn on with permanent marker just below each shard to aid in navigation when aiming the laser

The NAA results presented here focus on elements of importance for characterization and discrimination of archaeological pottery. An ochre-optimized NAA procedure could use different irradiation and counting parameters and different or additional standard reference materials for comparator method data reduction. While NAA method parameters may be refined specifically for ochres, the routine pottery

parameters have been successfully used since at least the mid-2000s and NAA of ochre is a mature technique available from MURR to any party submitting samples for elemental characterization.

NAA was carried out using preparation and instrumental methods described at length in Glascock (1992), Glascock and Neff (2003, Section 4.3), and Zipkin *et al.* (2015, Supplementary Information Section 4). The analytical parameters use two sample irradiations and three counts on a high-purity germanium detector to collect a spectrum of emitted gamma rays. The first count uses a short irradiation of 5 s, decay of 25 min, and counting time of 12 min to measure Al, Ba, Ca, Dy, K, Mn, Na, Ti, and V. The second and third counts are done after a single long irradiation of 24 h. The second count occurs 7–9 days after irradiation for 30 min to measure As, Ba, La, Lu, Nd, Sm, U, and Yb. The third count is made at 22–28 days using counting times of 2.5 h and measures Ce, Co, Cr, Cs, Eu, Fe, Hf, Ni, Rb, Sb, Sc, Sr, Ta, Tb, Th, Zn, and Zr (Glascock 1992; *pers. comm.* Glascock). Results for all submitted samples were normalized to NIST (National Institute of Standards and Technology) SRM (standard reference material) 1633 series and SRM 688 standards during data reduction. The only deviation in this study from the standard NAA methods for clays and ceramics described in the works by Glascock and colleagues is that ochre sample masses analyzed were reduced by ~ 50% due to their high Fe content. Short irradiation samples were 75–85 mg instead of ~ 150 mg. Long irradiation samples were 95–105 mg instead of ~ 200 mg (Zipkin *et al.* 2015; *pers. comm.* Glascock). All NAA results and limits of detection (LOD) are reported in Supplementary Table 3 as provided to the authors by MURR. LODs for individual analyses were not provided; instead a single LOD for each element was included with the sample results. These LODs are estimates based on long-term monitoring of pottery measurements by NAA at MURR and are not specific to ochres or this particular batch of samples (*pers. comm.* Glascock).

Lithium Borate Fusion Methods

The fusion procedure, and the specific blend of flux used, was initially developed in collaboration with Katanax/SPEX Sample Prep of Quebec, Canada. The method proposed by Katanax was then adapted for use in the University of Illinois at Urbana-Champaign (UIUC) Department of Geology geochemistry laboratory. The key difference between the Katanax method and the one used here is that at UIUC fusion was done in high-purity graphite crucibles in a standard muffle furnace. Katanax uses platinum alloy (Pt-Au) crucibles and molds in an automated fusion fluxer which agitates vessels during fusion. The use of Pt-Au vessels and an automated fusion fluxer is optimal for high-throughput applications such as quality control in an industrial environment but is likely out of financial reach for many researchers in an academic setting.

Experimental samples and the United State Geological Survey (USGS) reference material BCR-2 were both fused at 10:1 flux to sample ratio using a pre-fused micro-bead flux blend composed of 49.75% LiT, 49.75% LiM, and 0.5% LiBr, purchased from Scancia (Quebec, Canada; 99.99% purity). The 1:1 ratio of LiT to LiM yields a flux in which Fe_2O_3 (hematite) is near its maximum solubility in a LiBo melt but which is also capable of dissolving common non-iron components of ochre such as silicates (Claisse and Blanchette 2004). This blend is a compromise that has some drawbacks. Calcium oxides are less soluble

than in a pure LiT flux. The presence of LiT flux in a melt of iron-containing sample material can also yield fusion products which stick strongly to crucibles and molds. Use of a LiBr NWA mitigated this issue in most of our experimental ochre fusions. The required ratio of NWA to flux will vary depending on the nature of the samples fused. Flux blends can be produced as needed in-house by mixing multiple powder reagents or can be purchased from a supplier in pre-blended form. Experimentation with various blends applied to a range of representative samples for the proposed project is suggested prior to purchasing or formulating large amounts of flux.

One gram of flux was added to a high-purity (2 ppm total metal impurity limit), 8.4 ml capacity, graphite crucible (SPEX Sample Prep), followed by 100 mg of sample powder nestled in the flux without touching the graphite (Fig. 2b). Empty crucible mass, crucible plus flux mass, and crucible plus flux and sample mass were all measured on an analytical balance and recorded. While crucibles were loaded, the muffle furnace was pre-heated to 1050 °C. A maximum of 8 crucibles were loaded to the furnace at once; samples were fused without any agitation (Fig. 2c). After 30 min of fusion, crucibles were removed using tongs and allowed to cool (Fig. 2d). Each fused bead was removed from the crucible and examined against a white LED handheld light to determine if a qualitatively homogeneous bead had been produced. Any bead that exhibited opaque particles or distinct banding of darker and lighter areas was shattered and fused a second time in a clean crucible.

After each fusion, the empty crucible was cleaned by removing any adhering glass with a metal spatula, abrading the entire inner surface using 320 grit extra-fine wet/dry sandpaper and deionized water (18.2 MΩ-cm resistivity) until smooth and with no visible trace of fusion product, and rinsing with deionized water a final time. Although graphite crucibles are typically marketed as disposable, particularly relative to platinum alloy vessels, it is possible to use graphite repeatedly for at least a dozen fusions with sufficient cleaning and monitoring of process blanks to detect cross-contamination. This is addressed further under "Analysis of LiBo Fused Glass Blanks for Contamination Detection."

After fusion to homogeneous glass, each bead was wrapped in paper and shattered using a steel hammer and anvil, and suitable shards were selected for embedding in epoxy. Shards were generally selected based on size and shape: shards 1.0 to 5.0 mm in maximum dimension and exhibiting a flat surface were chosen. A 25 mm internal diameter polytetrafluoroethylene (PTFE) ring mold was adhered to pressure sensitive double-sided adhesive tape on a backing of rigid cardboard. The exterior perimeter of the mold was sealed to the cardboard backing with a removable viscoelastic silicone polymer (Silly Putty™, Crayola LLC) to prevent leakage. Ring molds were produced in the UIUC machine shop using commercially available PTFE rods. Up to 24 shards were then mounted inside the mold on the tape. Prior to placement in the mold, each shard was briefly dipped in 100% ethanol and air-dried to remove any dirt or oil from handling and ensure a secure bond to the tape. It is not possible to directly label the shards so it is critical to draw a labeled diagram of shard positions in the mold during this process. Struers Inc. EpoFix cold-mounting transparent epoxy was freshly mixed and poured into the mold until all samples were fully submerged. The mold was covered with an inverted plastic beaker to reduce hardener evaporation and allowed to cure at room temperature for 24 h (Fig. 2e). Once cured, the epoxy mount was removed from the mold and sequentially manually polished using 23 μm, 9 μm, and 3

μm silicon carbide metallographic abrasive film and 1 μm alumina slurry on a felt pad (Pace Technologies), with ultrasonic cleaning in deionized water between each step. Figure 2f shows an epoxy mount ready for laser ablation; the fused bead shards appear green, indicating that fusion occurred in a reducing environment yielding FeO rather than Fe_2O_3 in the glass (Claisse and Blanchette 2004). Supplementary Fig. 1 also shows a whole fused bead embedded and roughly polished in cross-section.

EPMA Methods

Electron Probe MicroAnalysis was carried out at the University of Maryland at College Park, Advanced Imaging and Microscopy Laboratory on a fee-for-service basis. The following major and minor elements were measured in each LiBo fused sample using a JEOL JXA-8900 SuperProbe EPMA: Na, Mn, Ca, K, Al, Mg, Fe, Ti, and Si. Replicate EPMA measurements were made at three locations on each fused sample. The following conditions were employed for the analyses: accelerating voltage of 15 kV, sample current of 25 nA, and a beam diameter of 20 μm. Natural magnetite, ilmenite, and hornblende were used as standards for determining major and minor element concentrations. Raw X-ray intensities were corrected using standard ZAF (atomic number, absorption, and fluorescence) techniques. Element concentrations were calculated in percent weight as oxides. It was assumed that all samples were composed of 90.95% flux by weight (21.65% Li_2O, 62.88% B_2O_3, 0.42% Br) based on oxide weight of flux components, their representative proportions in the blend, and the 10:1 flux to ochre ratio. LODs were calculated separately for each analysis based on background measurements of peak size for each elemental analyte at the one sigma level. Measured percent oxide results below the relevant LOD were converted to zero in reported results. The flux element constants were then deleted from the data set, and the measured results for remaining elements of interest were multiplied by 11 to correct for flux dilution, yielding oxide percent weight values representative of whole ochre prior to fusion.

LA-ICP-MS Methods

Ablation was carried out at the University of Illinois Urbana-Champaign using a Photon Machines (Teledyne Cetac) Excite excimer (193 nm wavelength) laser ablation system. During ablation of reference materials and fused glasses, the laser system was adjusted to a fluence of ~ 6 J/cm^2, which achieved clean ablation of the material. The spot size was set at 65 μm for all sample ablations. The laser was set to 10 Hz, and line scans at a travel rate of 2 μm sec^{-1} provided a smooth signal. Fused samples were ablated using 60 s duration scan lines with 30 s for washout and baseline measurement between ablations. The ablated powder was then delivered to a Thermo Scientific iCAP Q single collector ICP-MS for trace element analysis using a He carrier gas. Prior to analysis, ICP-MS sensitivity was optimized using NIST SRM 612. Samples were analyzed using a helium collision gas (kinetic energy discrimination) in order to minimize polyatomic interferences.

The data acquisition protocol used an analytical sequence of between two and four initial analyses using SRM NIST 610 glass as the primary standard, followed by approximately 10 ablations of experimental LiBo fused samples, and then two replicate

analyses of NIST 610 as a bracketing standard. Three replicate ablations were done on each experimental sample. USGS BCR-2G (Jochum and Stoll 2008) and LiBo fused BCR-2 were used as secondary standards for quality assurance/quality control (QA/QC) and were analyzed consecutive to the bracketing analyses NIST 610 over the course of each run. It is important to note that the commercially available BCR-2G glass secondary standard is distinct from USGS BCR-2 powder which was fused in-house with LiBo using the same reagents and procedures as for ochre. BCR-2G was primarily monitored for long-term QA/QC purposes for the instrument, while LiBo fused BCR-2 was considered a matrix-matched secondary standard directly comparable to the fused ochre samples due to the composition of both being dominated by the flux. BCR-2G results are not discussed in this report and sections discussing BCR-2 results below refer exclusively to the LiBo fused secondary standard.

LA-ICP-MS data processing was done using the Iolite v3.61 software package (The University of Melbourne) in the Igor Pro programming environment (Wave Metrics) using the methods described in Paton *et al.* (2011) and Zipkin *et al.* (2015). LODs for all elements measured were calculated for each ablation according to the procedure described in Longerich *et al.* (1996), which is identified as the "Normal" method in Iolite. Baselines (background) were automatically selected in Iolite using total beam intensity, with selection parameters manually adjusted and selections inspected until a single baseline was associated with each ablation. Time resolved data from each ablation were integrated and reduced from counts per second (cps) to ppm concentrations using the trace elements data reduction scheme with ^{57}Fe as the internal standard. Fe concentrations used for data reduction were derived from the EPMA measurements of the fused beads; the three replicate EPMA analyses were averaged to yield a mean wt.% FeO value for each bead. The mean wt.% oxide was converted to mean elemental Fe concentration in ppm, and this was used as the internal standard value for all replicate ablations associated with a given bead. Elemental measurements by LA-ICP-MS were treated similarly to results from EPMA. First, the data set was scrubbed of observations that could not be reduced due to corrupt data or anomalous low signal. For all remaining observations, elemental concentrations were compared to the associated LOD for each element and each ablation. Below detection limit (BDL) concentrations were converted to zero, a process referred to as "censoring" the data set (Palarea-Albaladejo *et al.* 2014).

Results

Analysis of LiBo Fused Glass Blanks for Contamination Detection

The elemental concentration data underlying this manuscript are provided in Supplementary Table 2 (All EPMA results including BCR-2), Supplementary Table 3 (All NAA results), Supplementary Table 4 (LA-ICP-MS of BCR-2 only), and Supplementary Table 5 (LA-ICP-MS of ochres only). The only data not included pertain to the measurement of LiBo process blanks by LA-ICP-MS. In order to monitor for contamination of fusion products by the crucibles or the flux, process blanks ($N = 8$) were prepared and analyzed with the 36 fused ochre samples reported here. Process blanks consist of fusions done only with LiBo flux, produced and analyzed using the same

conditions as the experimental ochre samples. None of the replicate ablations of the process blanks associated with the ochre samples presented here, or from the 20 additional blanks produced among the ~ 200 fusions in the broader OLKARIA project, had concentrations above the LOD for all elemental analytes of interest measured by LA-ICP-MS. This indicates negligible contamination from impurities in the flux, the crucible graphite, or ochre residue in the crucibles.

Analysis of USGS BCR-2 for Analyte Reliability

Although BCR-2 is not an ideal quality control standard for use with ochres, it is a well-studied and widely available reference material with iron content (total Fe_2O_3 = 13.77%) within the range of earthy ochres. Standard reference materials that approximate the composition of earthy ochres are largely unavailable, in contrast to iron ores for which standards are widely available for use in the extractive industries. Among the only potentially applicable standards to earthy ochres is USGS GXR-1 (jasperoid), which has known issues with inter-bottle heterogeneity (Kane *et al.* 1992). Furthermore, as a basalt whole rock reference material, BCR-2 is relevant to analyses of Kenyan Rift geological ochres because many are derived from weathering of volcanic rocks (Zipkin *et al.* 2017). Table 2 presents summary results from LA-ICP-MS of LiBo fused BCR-2 and illustrates the reliability of the elements measured. Results in this table are sorted in descending order by the absolute magnitude of mean percent difference of measured concentrations from BCR-2 reference concentrations. Positive values for mean percent difference indicate that BCR-2 fused 10:1 with lithium borate flux was measured at a higher concentration than the consensus value listed in the GeoReM database (Jochum *et al.* 2005). Negative mean percent differences indicate that it was measured at lower concentrations than the GeoReM consensus value. Of 41 elements measured by LiBo LA-ICP-MS, 28 elements yielded mean values less than 10% different from the GeoReM consensus value. Of those elements, 13 differ by less than 5%, including 9 less than 2%. The best 9 elements include trace transition metals (Co, Hf, Ta), trace rare earth elements (Pr, Gd, Dy, Yb), and major elements (carbon group-Si, alkaline earth metal-Ca). Elements more than 10% different from the GeoReM consensus value were considered to be unreliably measured and are mainly excluded from statistical analyses seeking to distinguish among sources. Potassium is a borderline case at 10.7% mean difference from the consensus value; we elected to treat this as acceptable since potassium is a potentially interesting minor element.

Major and minor elements measured in BCR-2 by EPMA of fused glass are presented in Table 3. Values for % difference from GeoReM should be interpreted in the same way as in Table 2. EPMA yielded reliable or very reliable major element measurements for all elements except Mn. Knowing the reliability of EPMA on LiBo fused glass is important both for the sake of EPMA as a standalone technique and because of its role in LA-ICP-MS. EPMA and LA-ICP-MS generally excel in different areas; EPMA is used to measure major and minor elements (> 1% and 1 to > 0.1% by weight, respectively), while LA-ICP-MS is better at measuring minor and especially trace elements. There are of course exceptions; in this study EPMA measurement of Mn was notably unreliable (22% different from the consensus value in GeoReM, Table 3), while LA-ICP-MS measurement of Mn differed by 6.4% from the GeoReM value on average (Table 2). In addition to providing major and minor element

Table 2 Summary of analyses of LiBo fused BCR-2 by LA-ICP-MS for quality control/quality assurance

Isotope measured	GeoReM consensus value* (ppm)	LA-ICP-MS mean result (ppm, $N = 70$)	LA-ICP-MS standard deviation	LA-ICP-MS CV (%) (coefficient of variation)	LA-ICP-MS mean difference (%) from GeoReM
Most reliably measured elements (< 5% different from consensus value)					
^{157}Gd	6.811	6.80	0.67	9.9	− 0.2
^{173}Yb	3.392	3.41	0.40	11.7	0.5
^{43}Ca	50,843.83	51,400	2600	5.1	1.1
^{163}Dy	6.424	6.34	0.65	10.3	− 1.3
^{29}Si	252,417.06	256,200	16,300	6.4	1.5
^{181}Ta	0.785	0.773	0.065	8.4	− 1.5
^{59}Co	37.33	37.9	1.1	2.9	1.5
^{141}Pr	6.827	6.94	0.4	5.8	1.7
^{165}Ho	1.313	1.29	0.12	9.3	− 1.8
^{178}Hf	4.972	5.07	0.55	10.8	2.0
^{90}Zr	186.5	182	19	10.4	− 2.4
^{159}Tb	1.077	1.04	0.088	8.5	− 3.4
^{147}Sm	6.547	6.85	0.52	7.6	4.6
Reliably measured elements (< 10% different from consensus value)					
^{167}Er	3.67	3.44	0.34	9.9	− 6.3
^{175}Lu	0.5049	0.473	0.05	10.6	− 6.3
^{51}V	417.6	444	13	2.9	6.3
^{45}Sc	33.53	31.4	2.3	7.3	− 6.4
^{55}Mn	1522.582	1620	38	2.3	6.4
^{146}Nd	28.26	30.2	2.3	7.6	6.9
^{133}Cs	1.16	1.08	0.11	10.2	− 6.9
^{232}Th	5.828	6.23	0.62	10.0	6.9
^{169}Tm	0.5341	0.496	0.051	10.3	− 7.1
^{151}Eu	1.989	2.13	0.16	7.5	7.1
^{88}Sr	337.4	362	30	8.3	7.3
^{137}Ba	683.9	737	45	6.1	7.8
^{139}La	25.08	27.1	1.7	6.3	8.1
^{89}Y	36.07	32.9	3.3	10.0	− 8.8
^{140}Ce	53.12	57.9	2.8	4.8	9.0
Unreliable elements (> 10% different from consensus value)					
^{39}K	14,726.81	16,300	610	3.7	10.7
^{85}Rb	46.02	53.3	3.9	7.3	15.8
^{23}Na	23,145.938	26,900	2200	8.2	16.2
^{238}U	1.683	1.96	0.12	6.1	16.5
^{27}Al	71,343.03	84,900	3600	4.2	19.0
^{48}Ti	13,578.86	10,500	320	3.0	− 22.7
^{66}Zn	129.5	166	14	8.4	28.2
^{65}Cu	19.66	28	10	35.7	42.4
^{53}Cr	15.85	23.7	12	50.6	49.5

Table 2 (continued)

Isotope measured	GeoReM consensus value* (ppm)	LA-ICP-MS mean result (ppm, $N = 70$)	LA-ICP-MS standard deviation	LA-ICP-MS CV (%) (coefficient of variation)	LA-ICP-MS mean difference (%) from GeoReM
^{62}Ni	12.57	18.9	4.4	23.3	50.4
^{75}As	0.86	1.54	0.79	51.3	79.1
^{208}Pb	10.59	20.9	4.2	20.1	97.4
^{121}Sb	0.302	0.713	0.38	53.3	136.1

GeoReM database (Jochum *et al.* 2005) consensus reference values for BCR-2 are from the current version as of May 2018. Positive % difference from GeoReM values indicates that the analyte had an elevated concentration relative to the reference value; negative % differences indicate that the analyte was depleted relative to the reference value. Reliability of elements measured refers to absolute mean % difference of LA-ICP-MS results from GeoReM consensus values.

*We use the term "consensus value" here but on the GeoReM website "preferred value" is used.

NM = not measured

concentrations to complement LA-ICP-MS trace element results, an EPMA measured major element (in this case, Fe) can be used as the internal standard element for LA-ICP-MS data reduction. Although Fe was not the most reliably measured major element by EPMA, we elected to use it as the internal standard for LA-ICP-MS because ochre must contain iron. Other researchers may of course choose otherwise. Measurement of multiple major elements by EPMA will generate a range of options from among which to select the internal standard element for LA-ICP-MS.

Analysis of Kenyan Ochres by EPMA

Major and minor element results from EPMA will only be addressed briefly. Major elements in ochres can exhibit substantial intra-source variation, as illustrated by the error bars in Fig. 3 which indicate the range associated with the plotted values for mean

Table 3 Summary results for major and minor elements measured by EPMA in BCR-2 as LiBo fused glass

	%Na_2O	%MnO	%CaO	%K_2O	%Al_2O_3	%MgO	%FeO	%TiO_2	%SiO_2
GeoReM consensus value	3.12	0.1966	7.114	1.774	13.48	3.599	12.39	2.265	54
EPMA mean value ($N = 16$)	2.98	0.24	7.34	1.69	13.8	3.7	13.5	2.4	55.8
% difference from GeoReM	− 4	22	3	− 5	2	3	9	6	3
Standard deviation	0.21	0.092	0.2	0.11	1.3	0.2	0.46	0.24	4.9
Coefficient of variation (%)	7.0	38.3	2.7	6.5	9.4	5.4	3.4	10.0	8.8

N = 16 analyses with 8 replicates per fused bead. Results are compared to GeoReM (Jochum *et al.* 2005) consensus reference values for BCR-2 from the current version as of May 2018. Positive % difference from GeoReM values indicates that the analyte had an elevated concentration relative to the reference value; negative % differences indicate that the analyte was depleted relative to the reference value.

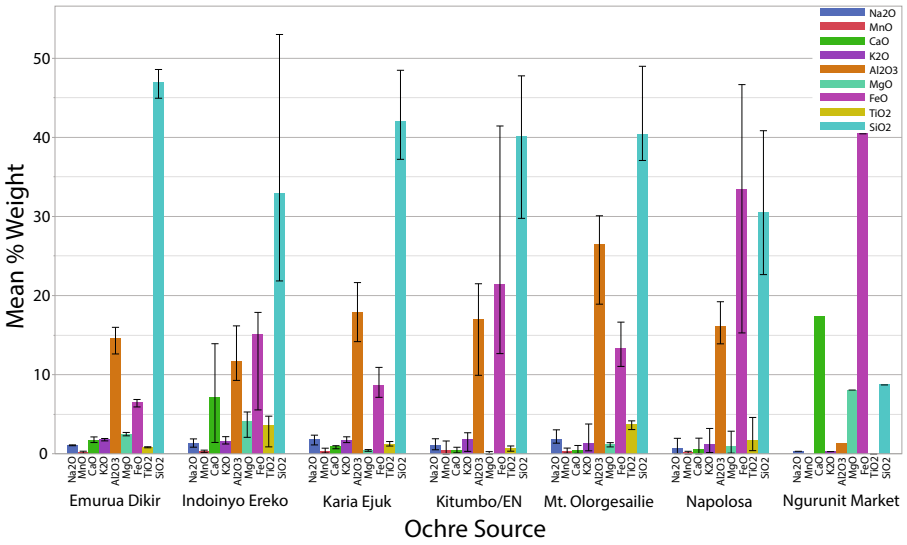

Fig. 3 Mean major element concentrations for sources as % weight oxides, as measured by EPMA on LiBo fused beads. Error bars indicate the range for each element based on individual EPMA measures for each source

percent weight oxide in each source. For this reason, we find that major and minor elements are generally not reliable for source discrimination or provenience analysis of archaeological ochres. The main reasons for obtaining measurements of such elements include (1) identifying exceptional cases where the sources under consideration are significantly and consistently different in major element composition, (2) characterizing matrix composition to inform subsequent reference material selection for LA-ICP-MS, (3) measuring potential internal standard elements for LA-ICP-MS data reduction, and (4) to collect a data set which may complement trace element measurements by LA-ICP-MS.

One notable finding based on major elements alone is that the single commercial ochre sample from the Ngurunit Market is unlike any of the geological sources considered. The Ngurunit ochre has more calcium, less aluminum, more magnesium, and less silica than samples from the six geologic sources. These major compositional differences, coupled with the high iron content, strongly suggest that the Ngurunit ochre was not collected directly from a geological source in our study area. It is more likely that the Ngurunit sample is derived from commercially manufactured iron oxide pigment for industrial use. Future ethnographic field work in Kenya will seek to elucidate the trade in and use of commercially available alternatives to ochre collected directly from geologic deposits.

Analysis of Kenyan Ochres by LA-ICP-MS and Data Exploration

The LA-ICP-MS data consist of 108 ablation results for 41 elemental variables, measured in 36 LiBo fused ochre samples. Observations were reduced to ppm from cps in Iolite with BDL observations automatically flagged during export. During laser ablation the amount of material removed may vary considerably, resulting in different

LODs for each analysis (Longerich *et al.* 1996). Separate LODs were calculated in Iolite for each ablation; Table 4 presents summary LODs and number of below detection limit observations for all measured isotopes. Table 5 lays out the data processing workflows used with the LA-ICP-MS results; the data set numbers refer to tabs in the Supplementary Table 5 spreadsheet where the data from each step in these workflows are provided in full. All descriptions of data processing, exploration, and statistical analysis that follow refer to the LA-ICP-MS results unless otherwise specified.

Rounded Zero Replacement and Transformations in Compositional Data

In the course of writing this manuscript, initially focused only on presenting a sample preparation technique, we found it impossible to ignore discussing how elemental concentration data are processed. Compositional data analysis is a field unto itself and is fundamentally important to archaeometry but is only occasionally addressed explicitly in geochemical provenience studies. For a very brief introduction, see the chapter by Buxeda i Garrigós (2018) in *The Encyclopedia of Archaeological Sciences*. We also highly recommend the Lowe *et al.* (2017) review of tephra and cryptotephra correlation practices for a detailed overview of compositional data analysis in an applied context. What follows below is a necessary digression from the rest of the manuscript for those interested in understanding our data processing choices and why they are of equal importance to laboratory methods for successful source discrimination.

Prior to conducting any statistical analysis, we sought to evaluate the multivariate distribution of our LA-ICP-MS elemental data. As discussed in Zipkin *et al.* (2017) and earlier noted by Baxter (1994), although many of the standard statistical techniques used for source discrimination are treated as being relatively robust to non-normal data, it is still useful to assess whether the data set in question deviates strongly from multivariate normality. A valuable tool for assessing multivariate normality is the MVN package for the R programming environment developed by Korkmaz *et al.* (2014). This tool is also available in a user-friendly interface online (http://www.biosoft.hacettepe.edu.tr/MVN/). MVN includes three tests: Mardia's multivariate skewness and kurtosis (Mardia 1970, 1974), the Henze–Zirkler empirical characteristic function test (Henze and Zirkler 1990), and Royston's multivariate Shapiro–Wilk test (Royston 1982, 1983). We applied all three tests to the complete ochre sample LA-ICP-MS data set (108 ablations, 41 elements) with BDL observations censored to zero as described under "LA-ICP-MS Methods" previously. This data set is identified as data set #1 in Table 5. All three MVN tests found that data set #1 is non-multivariate normal.

A base 10 logarithmic transformation helps to ensure that observations for all variables have similar orders of magnitude (Baxter 1994; Macdonald *et al.* 2018), which can both improve normality and prevent a small number of variables from overwhelming the contribution of other elements during multivariate analysis. A log10 transformation is particularly applicable to data sets such as ours which combine major, minor, and trace element measurements. One notable barrier to any logarithmic transformation is the inability to transform the value 0, such as for BDL observations that have been censored in data set #1. The issue of how to treat "rounded" (censored BDL measurements) versus "essential" (true zeroes, such as % mineral type where one

Table 4 Summary of limits of detection and below detection limit observations for LiBo LA-ICP-MS of ochres

Element	Mean LOD (ppm, $N = 108$)	# below LOD analyses (% BDL)
Major and minor elements		
^{27}Al	4.5	0
^{43}Ca	80	18 (16.7%)
^{39}K	9.2	0
^{55}Mn	0.084	0
^{23}Na	19.4	11 (10.2%)
^{29}Si	630	0
^{48}Ti	0.045	0
Trace elements		
^{75}As	0.158	8 (7.4%)
^{137}Ba	0.008	0
^{140}Ce	0.0010	0
^{59}Co	0.009	0
^{53}Cr	0.155	3 (2.8%)
^{133}Cs	0.076	13 (12.0%)
^{65}Cu	0.0327	0
^{163}Dy	0.0017	0
^{167}Er	0.0062	0
^{151}Eu	0.0026	0
^{157}Gd	0.0021	0
^{178}Hf	0.003	0
^{165}Ho	0.0223	0
^{139}La	0.0010	0
^{175}Lu	0.0013	0
^{146}Nd	0.0063	0
^{62}Ni	0.123	6 (5.6%)
^{208}Pb	0.0176	0
^{141}Pr	0.0057	0
^{85}Rb	0.027	0
^{121}Sb	0.039	3 (2.8%)
^{45}Sc	0.066	1 (0.9%)
^{147}Sm	0.0054	0
^{88}Sr	0.0179	0
^{181}Ta	0.0019	0
^{159}Tb	*	0*
^{232}Th	0.0005	0
^{169}Tm	0.0004	0
^{238}U	0.0006	0
^{51}V	0.0127	1 (0.9%)
^{89}Y	0.0068	0
^{173}Yb	*	0*

Table 4 (continued)

Element	Mean LOD (ppm, $N = 108$)	# below LOD analyses (% BDL)
^{66}Zn	0.158	0
^{90}Zr	0.0066	0

N refers to the total number of ablations in the data set (3 per fused ochre sample = 108 analyses)

*For Tb and Yb, no variation in baseline (background) was measurable by LA-ICP-MS so the LOD could not be calculated by the Longerich *et al.* (1996) method in Iolite for these elements. This does not mean that the LOD is infinitely low, just that it is impossible to quantify the actual LOD.

BDL = below detection limit

category is not found at all) zeroes in compositional data has received considerable attention over the last few decades. A basic and traditional approach, termed "simple substitution" or just "substitution," involves replacing the rounded zero observations for a given variable with a constant positive value smaller than the applicable limit of detection (Palarea-Albaladejo *et al.* 2014). The replacement value is typically 50–75% of the LOD; 65% is recommended by Martín-Fernández *et al.* (2003) and Palarea-Albaladejo and Martin-Fernandez (2013) in discussions of more advanced replacement strategies. As noted by Sanford *et al.* (1993), Baxter (1994), and Martín-Fernández *et al.* (2003), among others, simple substitution risks biasing the data set toward those variables with multiple censored observations that have been replaced. There is no agreed upon threshold for how large a percentage of a data set can be composed of censored values before the use of simple substitution is unacceptable. Helsel (2012), a work on censored data in environmental science that advocates against substitution, states that United States Environmental Protection Agency has considered it acceptable for up to 15% of a data set to be composed of censored values before simple substitution is not viable.

Aitchison, (1986) additive replacement, Fry *et al.* (2000), modified Aitchison, Martín-Fernández *et al.* (2000, 2003), multiplicative simple replacement, and Palarea-Albaladejo and Martin-Fernandez (2013), multiplicative lognormal replacement have all proposed alternatives to simple substitution. The chief advantage of the modified Aitchison and multiplicative replacement strategies is that they preserve the ratio relationship among the variables. Although a mathematical explanation of rounded zero replacement is beyond the scope of this work, we will address some aspects to elucidate our data processing choices. Advanced methods that seek to preserve the ratio relationship among variables rely upon a "closure operation." The principle of closure is fundamental to compositional data analysis and has presented challenges far beyond rounded zero replacement for decades (Skala 1979; Aitchison 1984). Closure in this context refers to the property that compositional data are parts of a whole (Aitchison 1986). This whole, or constant sum, may be 1 (proportional data), 100 (percent data), or 1,000,000 (ppm data), for example. Rounded zero replacement strategies that employ a closure operation require that the values of all variables measured in each analysis add to a known constant sum. The Martín-Fernández *et al.* (2000) multiplicative simple replacement method can be easily implemented in the free compositional data analysis software package CoDaPack (Thío-Henestrosa and Martín-Fernández 2005; University of Girona, http://www.compositionaldata.com/) using a closure operation that requires

Table 5 Data processing steps undertaken for LiBo LA-ICP-MS observations to address rounded zeroes (censored BDL observations) and non-multivariate normal data

Data processing workflow		Data set number (Tab in SI Table 5)	Data set description	Number of variables included	Variable units and format	Multivariate Normal?
A	B					
		1	All measured elements, with Below Detection Limit (BDL) observations as rounded zeroes	41	ppm	No
		2	From data set #1, all elements, with BDL observations as 65% of associated Limit of Detection	41	ppm	No
		3	From data set #2, with all elements standardized to associated mean Fe content measured by EPMA for each fused sample	41	Element X ppm/Mean Fe ppm	No
		4	From data set #3, with all variables log10 transformed	41	Log10(Element X ppm/Mean Fe ppm)	No
		5	From data set #4, variables limited to elements listed as "Most reliably measured" and "Reliably measured" in Table 2, plus potassium (K)	29	Log10(Element X ppm/Mean Fe ppm)	No
		6	From data set #5, variables further limited to those elements that have a positive significant correlation with Fe content from Pearson product-moment correlation at α=0.1 (see tab 2, SI Table 5)	5	Log10(Element X ppm/Mean Fe ppm)	No
		7	From data set #3, with all variables centered logratio transformed in CoDaPack	41	CLR(Element X ppm/Mean Fe ppm)	Unable to calculate tests: system is computationally singular
		8	From data set #7, variables limited to elements listed as "Most reliably measured" and "Reliably measured" in Table 2, plus potassium (K)	29	CLR(Element X ppm/Mean Fe ppm)	No
		9	From data set #8, variables further limited to those elements that have a positive significant correlation with Fe content from Pearson product-moment correlation at α=0.1 (see tab 2, SI Table 5)	5	CLR(Element X ppm/Mean Fe ppm)	No

a user-provided value for "closure to" (the constant sum). For the geochemical data considered here, we do not consider rounded zero replacement with closure to be viable. To specify closure to 1,000,000 ppm for all of the major, minor, and trace elements measured in a given analysis is to assume that we measured all elements present in the sample (*e.g.*, carbon, phosphorous, and sulfur were not measured) and

that we can treat all elements as reliably measured (demonstrated to be false in Table 2). In the future, we may explore applying multiplicative replacement to ochre elemental data from the standpoint that closure for *full composition* data sets is not viable. The alternative is to attempt to normalize a subset of elements to a different constant sum as suggested by Palarea-Albaladejo and Martin-Fernandez (2013). At this time, we do not believe it is advisable to apply this approach since there is little consensus in the literature on which elements are diagnostic for provenience studies of ochre (MacDonald *et al.* 2018).

For ochre data set #1, a total of 64 BDL observations were censored to 0, out of a total of 4428 observations (41 elements × 108 ablations). Table 4 and Supplementary Table 5, spreadsheet tab 1 show where the censored BDL observations are concentrated in this data set. Ca has 18 BDL out of 108 observations, Cs 13 out of 108, Na 11 out of 108, As 8 out of 108, Ni 6 out 108, Cr 3 out of 108, and Sb 3 out of 108. No other element has greater than 1 BDL observation each. In light of the very small proportion of BDL observations overall (1.45% of all observations) and tolerable proportion of BDL observations for specific elements (16.67% for Ca, 12.04% for Cs, 10.19% for Na, < 10% for all others), we elected to use simple substitution with 65% of the applicable LOD as the replacement value. This yielded data set #2 (Table 5 and Supplementary Table 5, spreadsheet tab 2) which forms the basis for all further standardized and transformed variations that follow. The simple substitution of BDL observations with positive values did not significantly affect multivariate normality; data set #2 remained non-normal.

Data set #2 possesses positive values for all observations, facilitating logarithmic transformations and additional data processing steps. In the case of a data set that violates multivariate normality, we recommend applying some or all of the following options: (1) standardizing all observations to Fe concentration (Popelka-Filcoff *et al.* 2007; Dayet *et al.* 2016; MacDonald *et al.* 2018); (2) applying log10 (Baxter 1994), additive or centered logratio (Aitchison 1986), or isometric logratio (Egozcue *et al.* 2003) transformations; and (3) limiting the elemental variables under consideration using explicitly defined criteria. The above steps can be applied independently or consecutively as needed for both improving data set normality and achieving source discrimination. This is not a novel approach: Popelka-Filcoff *et al.* (2008) used log10 transformed and Fe-standardized NAA data to characterize ochre sources in southern Arizona. Standardizing elemental concentrations to Fe concentration such that the data set for statistical analysis is composed of "Element X ppm/Fe ppm" ratios can be especially helpful for studies that feature substantial intra-source and inter-source variation in major element composition (Eiselt *et al.* 2011; MacDonald *et al.* 2018).

As originally presented by Popelka-Filcoff *et al.* (2008), iron standardized concentrations were only used for elements that were found to have a significant positive correlation with iron concentration (the "iron oxide signature", discussed further below). As noted earlier, the present study features a very diverse range of ochres with iron content ranging from FeO ~ 5.6 through ~ 46.7% (Fig. 3). Like MacDonald *et al.* (2018), we decided to standardize all elements to iron content, in this case using the mean percent weight FeO measured by EPMA for each LiBo fused sample converted to ppm elemental Fe. We applied this step to generate data set #3, which was also non-normal. At this stage, our data processing workflow divided; workflow A applied a log10 transformation to the Fe standardized data set #3, while workflow B applied a

centered logratio transformation using CoDaPack. We address workflow A first below. Data set #4 is both Fe standardized and log10 transformed (log10(Element X ppm/Mean Fe ppm)) but remains non-normal according to all MVN tests. Having failed to achieve normality with standardization and transformation, we began limiting the variables under consideration. Data set #5 is limited from all 41 LA-ICP-MS measured elements to the 29 most reliably measured elements based on the calculated BCR-2 mean difference from the GeoReM consensus value (Table 2, potassium and above included in data set #5). While the specific threshold for excluding variables from consideration is left to the judgment of the analyst, applying this step regardless of data set normality is important to ensure that any interpretations are based on reliably collected data. Despite these measures, data set #5 remained non-normal.

In the final step of workflow A, we limited the variables under consideration to the iron oxide signature elements that are also among the most reliably measured by LA-ICP-MS. We returned to data set #2 (BDL substituted, with no standardization or transformation) and calculated the Pearson product-moment correlation (Pearson's r: the correlation coefficient) between each element measured by LA-ICP-MS and the mean Fe content measured by EPMA for each fused ochre sample. Correlations and *p* values at 90% confidence are provided in spreadsheet tab 2 , Supplementary Table 5. We found that only eight elements exhibit a significant positive correlation with iron concentration: Sc, V, Cr, Zr, Sb, Hf, Pb, and Th. These elements comprise the iron oxide signature of the ochres; they are statistically associated with iron content and are assumed to be related to the source of iron in the ochre as opposed to non-iron dilutants such as silicates and clay minerals (Popelka-Filcoff *et al.* 2007). While some studies have emphasized making source discrimination and provenience determinations for ochres based primarily or solely upon the iron oxide signature elements (*e.g.*, Popelka-Filcoff *et al.* 2008; Eiselt *et al.* 2011; Dayet *et al.* 2016), we recommend treating all measured elements as of equal potential usefulness at the outset of data analysis. Zipkin *et al.* (2017) and MacDonald *et al.* (2018) are two recent ochre geochemistry studies that used a more inclusive elemental "fingerprinting" approach which did not exclude any elements *a priori*. Of the eight iron oxide signature elements here, five were included among the best measured elements in data set #5: Sc, V, Zr, Hf, and Th. We tested multivariate normality for data set #6, which includes only those five elements, and found that it remained non-normal.

Workflow B begins with data set #3 which was loaded to CoDaPack for transformation using an alternative approach to log10. The centered logratio (CLR) transformation is the logarithm of the input values weighted by the average of all variables in the data set (Aitchison 1986). More precisely, CLR is a log ratio contrast between the value of any one variable and the geometric mean of the compositional vector. The CLR transformation has been used with ochre compositional data in at least one previous study (Dayet *et al.* 2014) but has not yet been widely adopted in this area of archaeometry. CLR and other features of CoDaPack are explained in detail in Thío-Henestrosa and Martín-Fernández (2005). The transformation of data set #3 yielded data set #7, with 41 variables in the form CLR (Element X ppm/Mean Fe ppm). For this set, the MVN tool from Korkmaz *et al.* (2014) repeatedly produced an error for all three tests and was unable to indicate whether multivariate normality was achieved. Data sets #8 and #9 reproduced the steps taken to generate #5 and #6: limiting the variables under consideration to the 29 best measured elements and the 5 best measured iron oxide

signature elements respectively. The CLR transformed version of these sub-composition data sets remained non-normal. We have highlighted our failure to generate a multivariate normal data set using some of the commonly applied methods because this is not an uncommon occurrence during elemental chemistry studies of ochre in the experience of the authors. Non-normal distributions and sets containing BDL observations should not be prohibitive barriers to source discrimination or provenience analysis unless the statistical tests applied are shown to be highly sensitive to deviations from normality or the presence of BDL substituted data. Data processing can and should be tailored to the objective of a given project so long as the steps taken and rationale underlying them are made explicit as we have sought to do here.

Bivariate Data Exploration

The simplest, but perhaps most time-consuming, way to explore elemental data is to generate a series of bivariate plots comparing all possible combinations of reliably measured elements for all collected observations (*e.g.*, a scatterplot matrix, Lowe *et al.* 2017). This is the way provenience analysis often begins; for some materials like obsidian, it may also be the way it ends. For example, in Brooks *et al.* (2018), plotting concentrations of the elements Y and Zr on an x-y graph was effective at discriminating Middle Stone Age obsidian artifacts from Olorgesailie, Kenya, into six groups corresponding to known geological deposits. For ochre, this approach is usually insufficient for source or artifact group discrimination, but it can help identify both useful elements to include in multivariate analyses and elements that are correlated with one another and likely to prove redundant in such analyses. Bivariate elemental plots, and all other graphical and quantitative analyses described below, were produced in JMP 13.2 (SAS Institute Inc.).

Contrary to much of our previous experience, a major source discrimination finding from this project is based on a simple bivariate plot. As shown in Fig. 4, it is possible to differentiate among all the geological source groups and the commercial ochre sample using a plot of Fe-standardized strontium concentrations vs standardized concentrations of the rare earth element (REE) hafnium extracted from data set #3. Neither strontium nor hafnium as measured by LiBo LA-ICP-MS had any below detection limit values, so this plot does not include any rounded zeroes or observations replaced using simple substitution (Table 4, Supplementary Table 5). In addition, both Sr and Hf were reliably measured according to monitoring of the LiBo fused BCR-2 secondary standard (Table 2). An important feature of Fig. 4 is the use of elemental ratios standardized to Fe content; earlier versions of this biplot that used non-standardized ppm values from data set #2 were less effective at producing non-overlapping normal density ellipses.

The plotted points in Fig. 4 suggest that intra-source variability in trace element concentrations, independent of iron content, may be an issue. For example, the Indoinyo Ereko and Karia Ejuk source groups show a wide range of Fe-standardized strontium content. Adding new samples and sources in the future could reduce the usefulness of this two-element plot if high strontium variability leads to an inability to visually distinguish between group boundaries. The inset biplot in Fig. 4 illustrates a possible remedy. By log10 transforming the elemental ratio variables, the graphic representation of intra-source variability can be manipulated to emphasize different groups. The inset plot highlights variability within the Napolosa source while

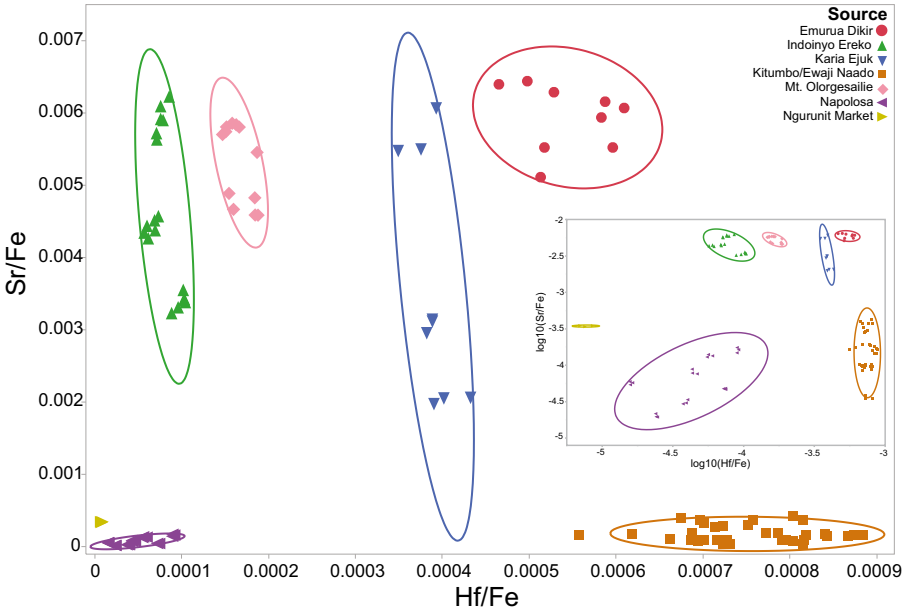

Fig. 4 Bivariate plot of strontium concentrations vs hafnium concentrations for ochre measured by LA-ICP-MS, both standardized to mean iron content in each LiBo fused bead as measured by EPMA. Sr and Hf data from all 108 ochre sample LA-ICP-MS analyses collected in this study are included in the plot. The plot also depicts non-overlapping bivariate normal 90% density ellipses for each ochre source group. The inset biplot shows the same two ratio variables log10 transformed

simultaneously reducing clutter from Indoinyo Ereko and Karia Ejuk. The Sr/Fe vs Hf/Fe biplot and its log transformed variant are highly effective first steps toward upholding the Provenience Postulate (Weigand *et al.* 1977). However, since these plots are only based on two elements of 41 measured, we consider them insufficient as standalone methods for source discrimination.

Multivariate Data Analysis

Following bivariate data exploration, we applied a standard multivariate statistical technique, principal components analysis (PCA), to the LiBo LA-ICP-MS data set. PCA is a dimension reduction method that facilitates the visualization of complex multivariate relationships in two- (or three-) dimensional space while maximizing the amount of variation represented. PCA and the related canonical discriminant analysis (CDA) are discussed in detail in the context of ochre in Zipkin *et al.* (2017); a more in-depth and general overview may be found in Baxter (1994). The elemental fingerprinting approach, as applied here, entails running an initial PCA using most or all of the reliably measured elements and identifying which variables have the greatest discriminatory power. If a PCA using this potentially large number of variables proves ineffective, redundant variables or weakly explanatory variables can be eliminated from consideration based on their eigenvectors and the loading matrix. PCAs using specific variables identified by other explicitly defined criteria, such as the iron oxide signature, are also applicable. Figure 5 illustrates the first PCA using the 29 elemental

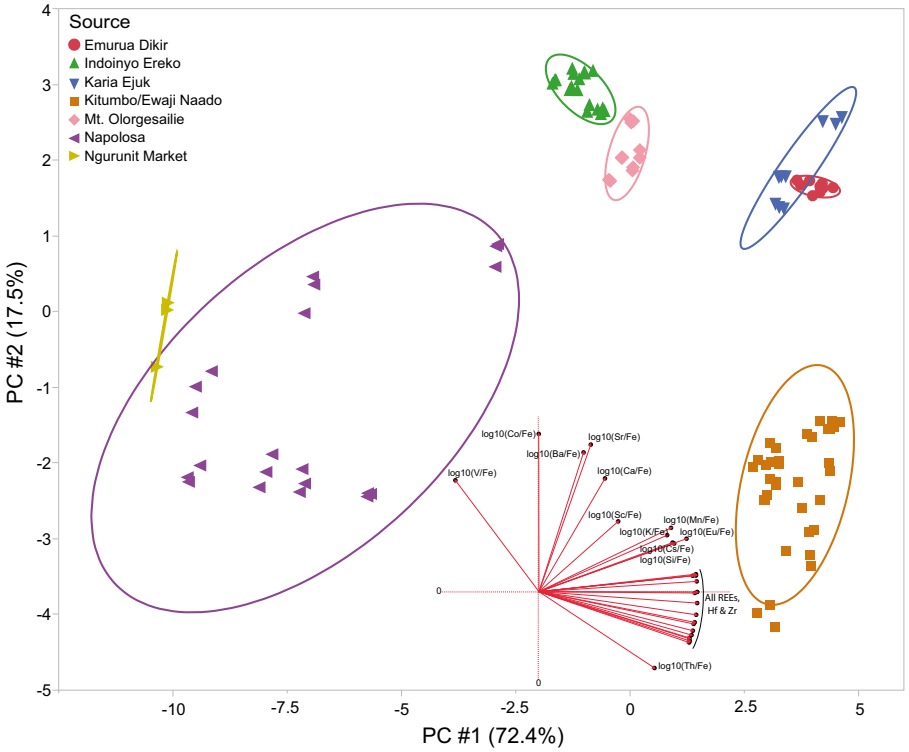

Fig. 5 Principal components analysis biplot (PC1 vs PC2) generated using data set #5 (Fe standardized, log10 transformed) with the 29 best measured elements by LA-ICP-MS. The inset plot of eigenvectors shows rays emanating from the origin (0,0) in the larger biplot and illustrates correlations among elements and between elements and PCs. The plot also depicts bivariate normal 90% density ellipses for each ochre source group. The axis labels show percent variation explained by each principal component

variables in data set #5 (concentrations standardized to Fe, log10 transformed). The inset eigenvector rays show that most of the REEs behave similarly; they, along with Hf and Zr, cluster together in a positive correlation with PC1. Sr and Ba are nearly orthogonal to most of the REEs and are positively correlated with PC2. This analysis is moderately effective at discriminating among source groups except for the overlapping density ellipses of Karia Ejuk and Emurua Dikir. One of the three replicate analyses of the Ngurunit Market ochre samples overlaps with the Napolosa source ellipse, but since the market-bought ochre effectively represents an unknown rather than a source (for geological provenience purposes), this should not be considered a weakness of the analysis.

We then refined our multivariate analysis of the sources to produce fully non-overlapping groups. Figure 6 shows a PCA using the five significant iron oxide signature elements (Sc, V, Zr, Hf, and Th) standardized to iron content but not otherwise transformed. The Fe-oxide signature PCA was highly effective at separating all source groups, with most of the inter-group variation occurring along the x-axis (PC1) which is dominated by vanadium, hafnium, zirconium, and thorium. Scandium, which primarily contributes to PC2 on the y-axis is less important in this analysis; if the y-axis was collapsed, most source groups would remain non-overlapping or overlap to a minimal extent. In light of the relative unimportance of scandium here, we proceeded

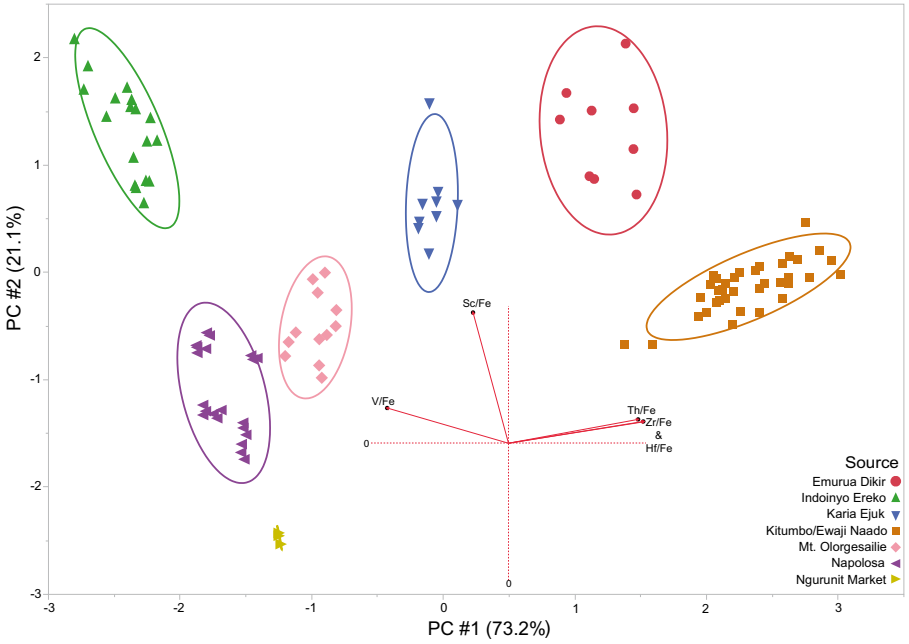

Fig. 6 Principal components analysis biplot (PC1 vs PC2) generated using the five iron oxide signature elements for the LA-ICP-MS observations: Sc, V, Zr, Hf, and Th. Concentrations were Fe standardized but not transformed. The inset plot of eigenvectors shows rays emanating from the origin (0,0) in the larger biplot and illustrates correlations among elements and between elements and PCs. The plot also depicts bivariate normal 90% density ellipses for each ochre source group. The axis labels show percent variation explained by each principal component

with one further refinement of this PCA. We replaced scandium with the non-iron oxide signature element strontium due to its utility in earlier steps of data exploration (*e.g.*, Figure 4) and used the Fe standardized and log10 transformed versions of these five variables. This PCA, shown in Fig. 7, complements the previous analysis by more effectively separating the Kitumbo/Ewaji Naado and Napolosa sources from the other groups. In both the Fe-oxide signature (Fig. 6) and transformed partial Fe-oxide signature (Fig. 7) PCAs, the Ngurunit ochre sample is found to be non-overlapping with any of the geologic source groups, further supporting the interpretation that it is a manufactured product distinct from the other, natural, ochres considered and is readily identifiable by its unique composition.

Comparison of Source Discrimination to the NAA Data Set

Having demonstrated that the LiBo fusion and LA-ICP-MS derived data permit effective source discrimination, we turned our attention to the NAA data set of 36 whole ochre sample results. The NAA dataset comprises 33 elemental variables: Al, As, Ba, Ca, Ce, Co, Cr, Cs, Dy, Eu, Fe, Hf, K, La, Lu, Mn, Na, Nd, Ni, Rb, Sb, Sc, Sm, Sr, Ta, Tb, Th, Ti, U, V, Yb, Zn, and Zr. Thirty-six bulk ochre samples were each measured once for these elements, yielding 1188 observations. We treated all elements measured by NAA as reliable for two reasons. First, NAA has long been considered a mature technique for which all systematic sources of error have been identified and

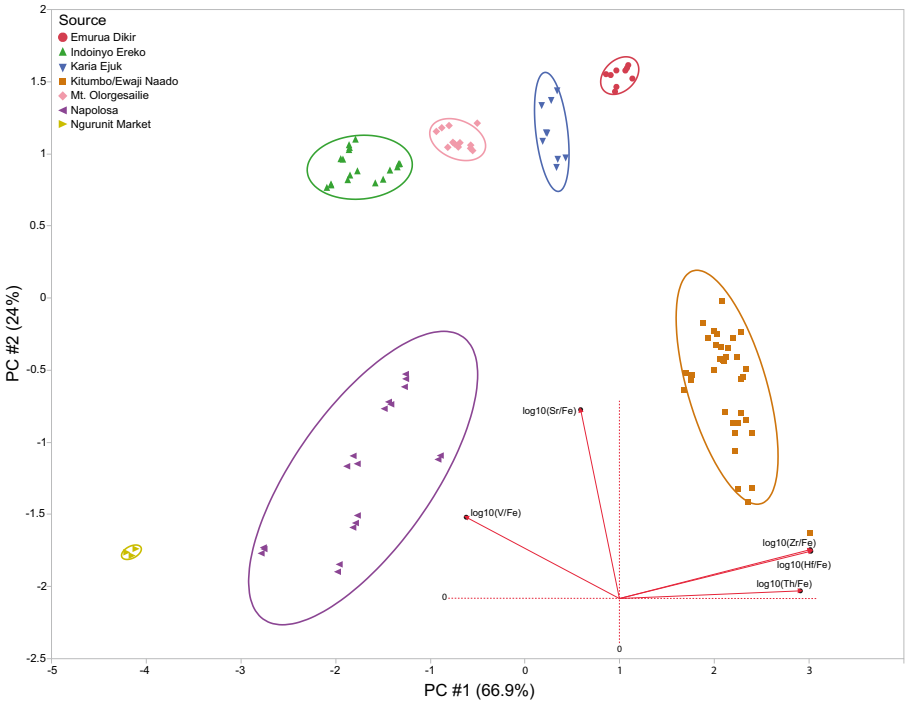

Fig. 7 Principal components analysis biplot (PC1 vs PC2) of LA-ICP-MS data generated using a modification of the iron oxide signature elements from Fig. 6. Scandium was replaced by the non-Fe oxide signature element strontium, and all variables were both Fe standardized and log10 transformed. The inset plot of eigenvectors shows rays emanating from the origin (0,0) in the larger biplot and illustrates correlations among elements and between elements and PCs. The plot also depicts bivariate normal 90% density ellipses for each ochre source group. The axis labels show percent variation explained by each principal component

appropriate methods developed to mitigate those errors. It remains indispensable in the development of standard reference materials and new analytical techniques (Moens and Dams 1995; Brown and Milton 2005). Second, MURR does not provide results for their own analyses of quality control standards to external parties submitting samples for analysis. The MURR lab does of course include standards for quality control with each batch of samples to be irradiated, such as NIST SRM 688 (basalt) and the in-house Ohio Red Clay standard originally prepared by Harbottle (1976), and uses these to correct data as necessary (Glascock and Neff 2003). The NAA data produced by MURR and provided to external parties are thus expected to be usable as received.

The NAA results provided in Supplementary Table 3 include multiple tabs that, like the LA-ICP-MS results in Supplementary Table 5, present results with BDL observations censored to 0 (tab 1), simple substitution of rounded zeroes using 65% of the applicable estimated LOD (tab 2), Fe standardization using the Fe values measured by NAA (tab 3), and log10 transformation (tab 4). As reported by MURR, 108 observations possessed negative concentrations; these represented BDL measurements which we treated in the same manner as those in the LA-ICP-MS data set. We attempted to discriminate among the ochre sources and commercial ochre sample using both iron oxide signature and elemental fingerprinting approaches to variable selection, as was done previously. We first calculated the Pearson product-moment correlation for each

measured element with iron using both the BDL as 0 and BDL with simple substitution data sets (tab 2). We compared the two sets of correlations using a matched pair t-test to ensure that they were not significantly different; this was necessary because the NAA LODs (and the substitution values based on them) are estimates. The test found no significant difference at 95% confidence ($N = 32$ elements excluding iron, t-ratio = −1.64443, Prob > |t| = 0.1102), indicating that replacing BDL observations with 65% of the estimated LOD will not change which elements comprise the iron oxide signature, relative to the default option of using BDL observations converted to 0. More simply, the same five elements exhibited positive correlations with Fe at 90% confidence for both the BDL as 0 and BDL substituted data sets.

The iron oxide signature elements include As, Cr, Sb, Th, and V; all have a significant positive correlation with Fe at 90% confidence. Of these, As and V were unsuitable for use in statistical analysis because they contained 22 and 13 BDL observations, respectively, out of 36 observations total for each element. As a result, the iron oxide signature approach to source discrimination using PCA is not tenable for the NAA data set with just the remaining three elements. Instead of the iron oxide signature, we turned to an elemental fingerprinting approach in which we initially used a PCA of all elements with less than 15% BDL observations (comparable to the 16.67% BDL for Ca in the LA-ICP-MS data, the highest of any element in that data set). This threshold disqualified As, Ca, Ni, Sr, and V. Fe standardized (using Fe measured by NAA) and log10 transformed data for the remaining 28 elements were used in a PCA. This PCA was mostly effective in differentiating among the sources. The density ellipses for the Emurua Dikir and Karia Ejuk sources overlapped in the biplot, as they did in the earlier LA-ICP-MS derived elemental fingerprinting biplot Fig. 5. We subsequently improved upon this by subtracting variables in a stepwise manner until the resulting PCA could discriminate among all geological sources.

The PCA shown in Fig. 8 uses 20 NAA measured elements in log10(X ppm/Fe ppm) form: Al, Ce, Co, Cr, Dy, Eu, Hf, K, Lu, Mn, Na, Rb, Sb, Sc, Sm, Ta, Tb, Th, Zn, and Zr. It is most comparable to the PCA in Fig. 5, which uses 29 LA-ICP-MS measured elements in the same data transformation format. Figures 5 and 8 PCAs have the following 14 elements in common: Ce, Co, Dy, Eu, Hf, K, Lu, Mn, Sc, Sm, Ta, Tb, Th, Zr. In both figures, the Ngurunit Market commercial ochre sample straddles the edge of the Napolosa group 90% density ellipse. However, the NAA data set in Fig. 8 successfully discriminates among Karia Ejuk and Emurua Dikir, which overlapped in Fig. 5. Notably, the NAA PCA includes two elements, Cr and Sb, which were excluded from statistical interpretation of the LA-ICP-MS data because they were considered unreliably measured. Ultimately, both LiBo LA-ICP-MS and bulk ochre NAA generated results which could be used to successfully discriminate among all 6 geologic sources in a functional demonstration of the strengths of both techniques for ochre elemental characterization.

Discussion

The method development work presented here demonstrates that lithium borate fusion of ochre for elemental analysis using EPMA and LA-ICP-MS is an effective approach to ochre source discrimination. The elemental measurements collected using NAA were

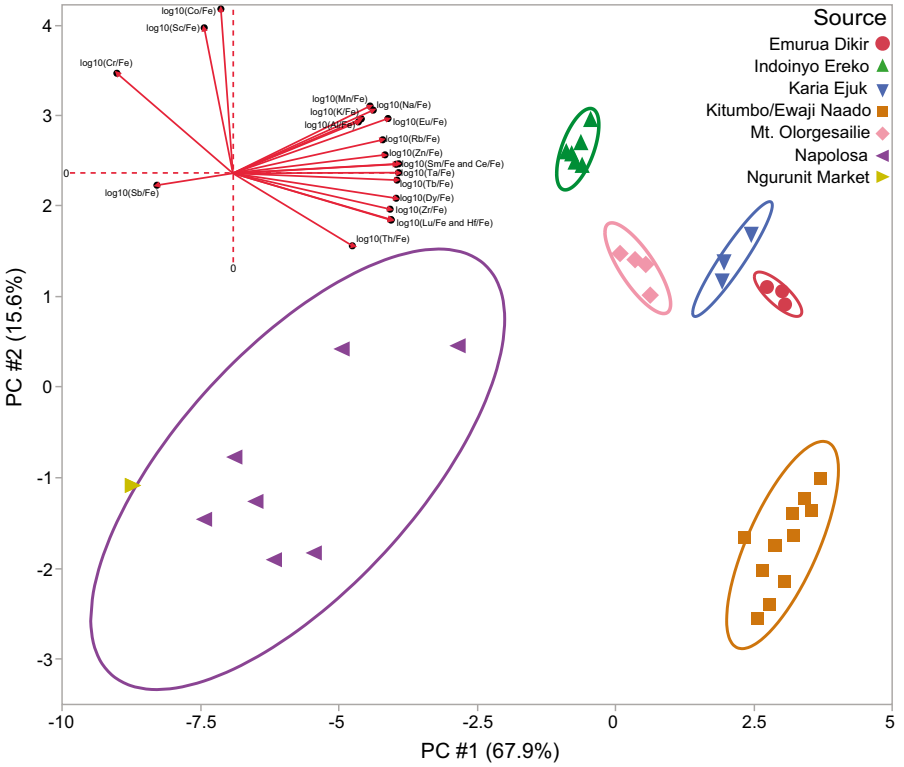

Fig. 8 Principal components analysis (PC1 vs PC2) for 20 of 28 elements with less than 15% BDL observations from the NAA data set. Concentrations were BDL substituted, Fe standardized, and log10 transformed prior to analysis; this data set is most comparable to LA-ICP-MS data set #5 from Table 5 (same data processing and similar number of variables). The plot also depicts bivariate normal 90% density ellipses for each ochre source group. The inset plot of eigenvectors shows rays emanating from the origin (0,0) in the larger biplot and illustrates correlations among elements and between elements and PCs. The axis labels show percent variation explained by each principal component

also able to discriminate among all sources. We argue that the laboratory methods in this work represent a valuable new approach to the analysis of ochre, particularly from the perspective of generating large data sets containing multiple replicate analyses per ochre sample and for producing prepared samples suitable for long-term storage and later study by other researchers to facilitate meta-analyses. Borate fusion also helps resolve multiple methodological issues specific to beam technique analysis of ochres.

This work was limited in scope and did not rely upon canonical discriminant analysis for distinguishing among sources, as was done in Zipkin *et al.* (2017). While we were able to uphold the Provenience Postulate (Weigand *et al.* 1977) using only bivariate plots and PCAs for the sources considered here, distinguishing among a larger number of sources and assigning artifact geologic provenience in future work will likely involve CDA. In contrast to PCA, discriminant analyses are quite sensitive to sample size. Harbottle (1976) suggests that the ratio of observations to variables should be between three and five in order to yield stable results. For an archaeological sourcing project in which CDA is expected to be used, fused solid-state samples may be subjected to many replicate chemical analyses in order to increase the number of

observations available for statistical evaluation. Such observations should be investigated both as individual ablation results and as mean results for each fused bead to determine the effects of a repeated measures data set versus an averaged data set that may suppress intra-specimen variation.

Replicate analysis of fused samples by XRF, SEM-EDS, EPMA, or LA-ICP-MS is of minor cost in time and money compared to NAA replicates and perhaps more importantly does not require additional destructive sample collection and preparation. LiBo fusion and repeated solid-state analysis is also likely to be more efficient than full acid digestion of ochre for solution ICP-MS and/or ICP-optical emission spectrometry, depending on the volume of solution consumed per analysis. The approach presented here is appropriate for application by archaeological scientists seeking direct control over chemical data collection and the ability to tailor methods to their own specifications. Having presented this method and its utility, we hope that others will adopt it, further refine it, and seek to validate it through inter-laboratory comparisons of LiBo fused standard reference materials and ochre samples. If lithium borate fusion preparation for solid-state analysis of ochre becomes widely used, we foresee the potential for both academic and cultural resource management archaeologists to process their own samples to the stage of embedding and polishing (Fig. 2f) before turning them over to university or commercial chemist collaborators for analysis with benchtop/laboratory instruments. As archaeologists increasingly apply XRF themselves using portable instruments, producing LiBo fused beads from experimental and reference materials for in-house collection of major and minor element data may become a routine feature of the archaeological science of ochre.

In *Physics and Chemistry of Borate Fusion* (2004), Claisse and Blanchette describe the major advantages of this approach to sample preparation for XRF analysis. Although we analyzed fused ochre beads using EPMA and LA-ICP-MS, these points still apply and represent solutions to concerns about the geochemical analysis of ochre using electron beam, ion beam, and laser microbeam methods raised by Killick (2015) and other authors. One important issue identified by Killick is the use of (or absence of) matrix-matched standards during analysis of solid-state materials. Ideally, absolute concentrations of elements in ochre would be determined by data reduction (cps to ppm) using a standard reference material with ochre-like elemental composition. Furthermore, the reference material should have comparable physical and material properties to the experimental samples, such as particle size, surface topography, and presence of free and chemically bound water. In a study using LA-ICP-MS on whole ochre, Scadding *et al.* (2015) raised similar limitations to those noted by Killick. They stated that LA-ICP-MS of whole ochre is effectively qualitative because of the variation in ablation efficiency between samples due to changes in sample matrix and analyte composition and the lack of matrix-matched standards. Although a pressed powder iron and manganese oxide-rich microanalytical reference material (FeMnOx-1, Jochum *et al.* 2016) became available a few years ago, it has not yet seen widespread adoption in archaeometry and lacks a long-term record of reported measurements by different laboratories that permit assessment of its homogeneity across pellets.

The use of lithium borate fused glasses for analysis of ochre by beam techniques represents an opportunity to resolve the issues surrounding matrix-matching comprehensively. Fusion removes all mineralogical and particle size heterogeneity effects, without requiring a full acid digestion process, by producing an amorphous glass. Free

and bound water are driven off by the temperatures at which fusion is done. The problem of analytical totals less than 100%, also noted by Killick (2015), can be mitigated by conducting loss on ignition (LOI) analysis of ochre samples prior to fusion to ensure that flux to sample ratios reflects only non-volatile elements that will be present after fusion. The ratio at which sample material and flux are fused effectively makes the ochre into a minor component of the resulting glass. Matrix effects deriving from differences in composition among experimental samples compared to an LiBo fused reference material will likely be negligible compared to the similar major element composition dominated by the flux (Claisse and Blanchette 2004). Finally, using LiBo fusion to produce in-house standards will facilitate improved data reduction and QA/QC procedures for solid-state analysis of ochres. A laboratory planning to use LiBo fusion on ochre samples can acquire USGS and other reference materials in powder form, which are more readily available and diverse in composition than certified glasses, and produce beads fused at the same ratio and using the same flux as the ochre samples. In addition to the adoption of pre-fusion LOI analysis, the identification and use of suitable iron-rich powder reference materials to produce LiBo fused standards represents the next step of refining this method for inter-laboratory validation and widespread application.

This experimental study exclusively addressed geological or commercially available ochres for which minimizing sample mass was not an overriding concern. The same will be true in a large-scale endeavor to build a reference data set of elemental fingerprints for archaeologically relevant geologic ochre sources, such as our broader OLKARIA project. The next significant challenge will be to modify these procedures for application to archaeological ochre and conduct an "apples to apples" provenience comparison of elemental data for sources and artifacts collected using identical laboratory methods. While a 100 mg ochre sample was used for all fusion results reported here, the same 10:1 ratio has been successfully used by the authors to produce fused beads from 100 mg flux and 10 mg of ochre. The most notable anticipated barrier to reducing sample mass is unrelated to fusion itself. Use of smaller volume crucibles and precise measurement of flux and ochre with an analytical balance facilitates the successful fusion of beads far smaller than those typically made for XRF analysis, or those made here for LA-ICP-MS on a shattered bead shard.

As ochre mass for fusion is reduced, the major concern will be ensuring that the samples analyzed are representative of the original geologic source. As noted earlier, ochre encompasses a wide range of materials, and these can exhibit considerable intra-source variation in mineralogy and major element composition. The use of Fe-standardized concentration ratios during data analysis helps mitigate the effects of major element variation between samples from the same geologic source. However, it is unclear if data processing measures will be sufficient when analyzing discrete ochre artifacts which are themselves already analogous to a source sample through their original mining or collection. The preparation and analysis of ever smaller masses in a quest to minimize damage to artifacts will require experimentation using expendable geologic source samples to determine the optimal strategy for removing ochre from a specimen, homogenizing it, and analyzing it. For example, if multiple 10 mg sub-samples removed as intact chips or drilled powder from a large ochre hand specimen yield comparable elemental results to 10 mg and 100 mg sub-samples of the same whole hand specimen homogenized to powder before sub-sampling, then the analysis

of archaeological ochres may prove viable with this method. The application of subsampling protocols based on Gy's sampling theory (Gy 1998; Gerlach and Nocerino 2004) offers one path forward, though this will require refinement to the specific challenges of archaeological ochres.

Conclusions

Ultimately, we recommend a hierarchical approach to the chemical study of geological and archaeological ochre that begins with the least expensive, technically demanding, destructive, and potentially informative methods and proceeds to additional, more powerful, analytic techniques as needed. Portable XRF analysis of bulk ochre from geologic sources may be a useful first step that could prove effective for distinguishing among sources in some study areas if appropriate calibrations with reference standards are used. Even if this is not the case, these preliminary measurements can shed light on elements of interest and provide insight into major element composition which will inform parameters and standard reference material selection for subsequent instrumental methods.

Lithium borate fusion sample preparation using the procedure presented here produces samples that are suitable for analysis by multiple techniques such as XRF, SEM-EDS, EPMA, and LA-ICP-MS. By fusing ochre into glass, many of the obstacles posed by analysis of whole ochre in its collected state are eliminated. XRF, SEM-EDS, or EPMA of fused samples to measure major and minor elements will likely represent a considerable advance beyond the same techniques applied to whole ochre from the perspective of obtaining a reliable elemental fingerprint representative of bulk sample composition. If the data obtained at that stage are insufficient to discriminate among sources and assign artifact provenience, the results collected thus far are still useful. The fused samples can also be subjected to the most powerful technique, LA-ICP-MS, which generally requires the measurement of an internal standard element by an independent technique to yield fully quantitative results. One of the major elements measured earlier can be used as this internal standard during the data reduction process and others may be combined with the trace element results from LA-ICP-MS to produce an elemental fingerprint spanning much of the periodic table. The methods presented here amount to a standard operating procedure which other researchers may adopt or use as starting point to develop their own techniques. By making explicit our ochre-tailored sample preparation technique, and the choices made during data collection and processing, we aim to encourage other archaeological scientists to do the same and to facilitate the collection of high-quality data that can be combined across laboratories for meta-analyses that answer meaningful questions in anthropological archaeology.

Acknowledgments All EPMA measurements were taken by Dr. Philip Piccoli of the University of Maryland at College Park Department of Geology. All NAA measurements were made by staff of the Missouri University Research Reactor Archaeometry Laboratory. Mr. Benoit Bouchard of Katanax/SPEX SamplePrep assisted in the initial development of the LiBo fusion procedure for ochre.

We thank the Kenya National Commission for Science, Technology, and Innovation (NACOSTI), Republic of Kenya Ministry of Higher Education Science and Technology, and National Council for Science and Technology for research clearance (Permit No. NACOSTI/P/15/6102/6746). This work would not have been

possible without the efforts of our Maasai, Dorobo, and Samburu field guides, informants, and hosts (*ashe oleng*!), and John Munyiri of the National Museums of Kenya Archaeology Department. We also thank Ms. Mercy Gakii (National Museums of Kenya Cultural Heritage Department) and Mr. Matthew Magnani (Harvard University Department of Anthropology) for help in documenting ochre deposits and ethnography of traditional source exploitation and cultural practices.

Funding Information This project was supported by grants for ochre ethnography and source sampling in Kenya and geochemical characterization in the USA: National Science Foundation (NSF) SBE Interdisciplinary Postdoctoral Fellowship SMA-1513984 (Zipkin, Ambrose, Lundstrom), NSF Senior Archaeology Research Grant BCS-15-61176 (Zipkin, Ambrose), and Wenner-Gren Foundation Post-Ph.D. Research Grant 02628 (Zipkin). LA-ICP-MS was made possible by NSF Instrumentation and Facilities Grant EAR-1441465 (Lundstrom, Ambrose, Johnson, Guenthner).

References

Aitchison, J. (1984). The statistical analysis of geochemical compositions. *Mathematical Geology, 16*, 531–564.

Aitchison, J. (1986). *The Statistical Analysis of Compositional Data. Monographs on Statistics and Applied Probability*. London, Chapman, & Hall Ltd.

Arocena, J. M., Hall, K., & Meiklejohn, I. (2008). Minerals provide tints and possible binder/extender in pigments in san rock paintings (South Africa). *Geoarchaeology, 23*, 293–304.

Audouin, F., & Plisson, H. (1982). Les ocres et leurs témoins au Paléolithique en France: Enquête et expériences sur leur validité archéologique. *Cahiers du Centre de Recherches Préhistoriques Paris, 8*, 33–80.

Baxter, M. J. (1994). *Exploratory Multivariate Analysis in Archaeology*. Edinburgh: Edinburgh University Press.

Brandt, S. A., & Weedman, K. (2002). Woman the toolmaker: a day in the life of an Ethiopian woman who scrapes hides the old-fashioned way. *Archaeology, 55*, 50–53.

Brooks, A. S., Yellen, J. E., Potts, R., Behrensmeyer, A. K., Deino, A. L., Leslie, D. E., Ambrose, S. H., Ferguson, J. R., d'Errico, F., Zipkin, A. M., & Whittaker, S. (2018). Long-distance stone transport and pigment use in the earliest middle stone age. *Science, 360*(6384), 90–94.

Brown, R. J., & Milton, M. J. (2005). Analytical techniques for trace element analysis: an overview. *TrAC Trends in Analytical Chemistry, 24*, 266–274.

Buxeda i Garrigós, J. (2018). Compositional data analysis. In S. L. López Varela (Ed.), *The Encyclopedia of Archaeological Sciences*. https://doi.org/10.1002/9781119188230.saseas0103.

Chalmin, E., & Huntley, J. (2017). Characterizing rock art pigments. In D. David & I. J. McNiven (Eds.), *The Oxford Handbook of the Archaeology and Anthropology of Rock Art* (pp. 1–38). New York: Oxford University Press.

Chamberlain, N. (2006). Report on the rock art of south west Samburu District, Kenya. *Azania, 41*, 139–157.

Chaptal, M. (1809). Notice sur quelques couleurs trouvées à Pompeïa. *Mémoires de la Classe des Sciences Mathématiques et Physiques de l'Institut de France Année, 1808-1809*(1809), 229–235.

Claisse, F. (1957). Accurate X-ray fluorescence analysis without internal standards. *Norelco Reporter, 4*, 3–7.

Claisse, F. (2003). Fusion and fluxes. In Z. Mester & R. Sturgeon (Eds.), *Comprehensive Analytical Chemistry XLI* (pp. 301–311). Amsterdam: Elsevier.

Claisse, F., & Blanchette, J. S. (2004). *Physics and Chemistry of Borate Fusion: Theory and Application* (3rd ed.). Quebec: Katanax Inc..

Cornell, R. M., & Schwertmann, U. (2003). *The Iron Oxides: Structure, Properties, Reactions, Occurrences and Uses* (2nd ed.). Weinheim: Wiley-VCH.

d'Errico, F., Bouillot, L. D., García-Diez, M., Martí, A. P., Pimentel, D. G., & Zilhão, J. (2016). The technology of the earliest European cave paintings: El Castillo Cave, Spain. *Journal of Archaeological Science, 70*, 48–65.

Dart, R. A. (1968). The multimillennial prehistory of ochre mining. *Native Affairs Department Annual, 9*(7), 7–13.

Davy, H. (1815). Some experiments and observations on the colours used in painting by the ancients. *Philosophical Transactions of the Royal Society of London, 105*, 97–124.

Dayet, L., d'Errico, F., & Garcia-Moreno, R. (2014). Searching for consistencies in Châtelperronian pigment use. *Journal of Archaeological Science, 44*, 180–193.

Dayet, L., Le Bourdonnec, F. X., Daniel, F., Porraz, G., & Texier, P.-J. (2016). Ochre provenance and procurement strategies during the middle stone age at Diepkloof Rock Shelter, South Africa. *Archaeometry, 57*(5), 807–829.

Dizé, M. J. J. (1790). Analyse du cuivre, avec lequel les Anciens fabriquoient leurs Médailles, les instruments tranchans. *Observations sur la Physique, sur l'Histoire Naturelle et sur les Arts, 36*, 272–276.

Eggins, S. M. (2003). Laser ablation ICP-MS analysis of geological materials prepared as lithium borate glasses. *Geostandards and Geoanalytical Research, 27*(2), 147–162.

Egozcue, J. J., Pawlowsky-Glahn, V., Mateu-Figueras, G., & Barceló-Vidal, C. (2003). Isometric logratio transformations for compositional data analysis. *Mathematical Geology, 35*(3), 279–300.

Eiselt, B. S., Popelka-Filcoff, R. S., Darling, A., & Glascock, M. D. (2011). Hematite sources and archaeological ochres from Hohokam and O'odham sites in Central Arizona: an experiment in type identification and characterization. *Journal of Archaeological Science, 38*(11), 3019–3028.

Ellis, L. W., Caran, S. C., Glascock, M. D., Tweedy, S. W., & Neff, H. (1997). Appendix H: Geochemical and Mineralogical Characterization of Ocher from an Archaeological Context. In S. L. Black, L. W. Ellis, D. G. Creel, & G. T. Goode (Eds.), *Hot Rock Cooking on the Greater Edwards Plateau: Four Burned Rock Midden Sites in West Central Texas* (pp. 660–678). Austin: Texas Archeological Research Laboratory, University of Texas at Austin.

Falcone, R., Renier, A., & Verita, M. (2002). Wavelength-dispersive X-ray fluorescence analysis of ancient glasses. *Archaeometry, 44*(4), 531–542.

Farnsworth, M. (1951). Ancient pigments: particularly second century BC pigments from Corinth. *Journal of Chemical Education, 28*, 72–76.

Frahm, E. (2014). What constitutes an obsidian "source"?: Landscape and geochemical considerations and their archaeological implications. In C. Dillian (Ed.), *Twenty-Five Years on the Cutting Edge of Obsidian Studies* (pp. 49–70). International Association for Obsidian Studies.

Froment, F., Tournié, A., & Colomban, P. (2008). Raman identification of natural red to yellow pigments: ochre and iron-containing ores. *Journal of Raman Spectroscopy, 39*, 560–568.

Fry, J. M., Fry, T. R., & McLaren, K. R. (2000). Compositional data analysis and zeros in micro data. *Applied Economics, 32*(8), 953–959.

Geertz, C. (1973). *The Interpretation of Cultures*. New York: Basic Books.

Gerlach, R. W., & Nocerino, J. M. (2004). Guidance for obtaining representative laboratory analytical subsamples from particulate laboratory samples. US Environmental Protection Agency, Office of Research and Development, National Exposure Research Laboratory, Environmental Sciences Division. https://nepis.epa.gov/Exe/ZyPURL.cgi?Dockey=2000GTWM.txt. Accessed 6 Nov 2018.

Glascock, M. D. (1992). Characterization of archaeological ceramics at MURR by neutron activation analysis and multivariate statistics. In H. Neff (Ed.), *Chemical Characterization of Ceramic Pastes in Archaeology* (pp. 11–26). Madison: Prehistory Press.

Glascock, M. D., & Neff, H. (2003). Neutron activation analysis and provenance research in archaeology. *Measurement Science and Technology, 14*(9), 1516–1526.

Gosden, C., & Marshall, Y. (1999). The cultural biography of objects. *World Archaeology, 31*(2), 169–178.

Gray, A. L. (1985). Solid sample introduction by laser ablation for inductively coupled plasma source mass spectrometry. *Analyst, 110*, 551–556.

Gregoricka, L. A. (2014). Assessing life history from commingled assemblages: the biogeochemistry of intertooth variability in Bronze Age Arabia. *Journal of Archeological Science, 47*, 10–21.

Günther, D., Quadt, A. V., Wirz, R., Cousin, H., & Dietrich, V. J. (2001). Elemental analyses using laser ablation-inductively coupled plasma-mass spectrometry (LA-ICP-MS) of geological samples fused with Li2B4O7 and calibrated without matrix-matched standards. *Microchimica Acta, 136*(3–4), 101–107.

Gy, P. M. (1998). *Sampling for Analytical Purposes*. Chichester: Wiley.

Harbottle, G. (1976). Activation analysis in archaeology. In G. W. A. Newton (Ed.), *Radiochemistry: a specialist periodical report* (pp. 33–72). London: The Chemical Society.

Helsel, D. R. (2012). *Statistics for censored environmental data using Minitab and R*. Hoboken: John Wiley, & Sons.

Henshilwood, C. S., d'Errico, F., & Watts, I. (2009). Engraved ochres from the middle stone age levels at Blombos Cave, South Africa. *Journal of Human Evolution, 57*(1), 27–47.

Henze, N., & Zirkler, B. (1990). A class of invariant consistent tests for multivariate normality. *Communications in Statistics - Theory and Methods, 19*, 3595–3618.

Hovers, E., Ilani, S., Bar-Yosef, O., & Vandermeersch, B. (2003). An early case of color symbolism: ochre use by modern humans in Qafzeh Cave. *Current Anthropology, 44*(4), 491–511.

Huntley, J. (2012). Taphonomy or paint recipe: in situ portable x-ray fluorescence analysis of two anthropomorphic motifs from the Woronora Plateau, New South Wales. *Australian Archaeology, 75*(1), 78–94.

Ichikawa, S., & Nakamura, T. (2014). X-ray fluorescence analysis with micro glass beads using milligram-scale siliceous samples for archeology and geochemistry. *Spectrochimica Acta Part B: Atomic Spectroscopy, 96*, 40–50.

Jochum, K. P., & Stoll, B. (2008). Reference materials for elemental and isotopic analyses by LA-(MC)-ICP-MS: Successes and outstanding needs. In P. Sylvester (Ed.), *Laser ablation ICP-MS in the Earth Sciences: Current Practices and Outstanding Issues* (pp. 147–168). Quebec: Mineralogical Association of Canada.

Jochum, K. P., Nohl, U., Herwig, K., Lammel, E., Stoll, B., & Hofmann, A. W. (2005). GeoReM: a new geochemical database for reference materials and isotopic standards. *Geostandards and Geoanalytical Research, 29*(3), 333–338.

Jochum, K. P., Wilson, S. A., Becker, H., Garbe-Schönberg, D., Groschopf, N., Kadlag, Y., Macholdt, D. S., Mertz-Kraus, R., Otter, L. M., Stoll, B., & Stracke, A. (2016). FeMnOx-1: A new microanalytical reference material for the investigation of Mn–Fe rich geological samples. *Chemical Geology, 432*, 34–40.

Joyce, R. (2012). From place to place: provenience, provenance, and archaeology. In G. Feigenbaum & I. Reist (Eds.), *Provenance. An Alternate History of Art* (pp. 50–62). Los Angeles: Getty Research Institute.

Joyce, R. (2013). When is authentic? Situating authenticity in the itineraries of objects. In A. Guerds & L. Van Broekhoven (Eds.), Creating *Authenticity. Authentication Processes in Ethnographic Museums* (pp. 39–58). Leiden: Sidestone Press.

Kane, J. S., Siems, D. F., & Arbogast, B. F. (1992). Geochemical exploration reference samples GXR–1 to GXR–4 and GXR–6: evaluation of homogeneity based on high precision analyses. *Geostatistics Newsletter, 16*, 45–54.

Kiehn, A. V., Brook, G. A., Glascock, M. D., Dake, J. Z., Robbins, L. H., & Campbell, A. C. (2007). Fingerprinting specular hematite from mines in Botswana, Southern Africa. In M. Glascock, R. J. Speakman, & R. S. Popelka-Filcoff (Eds.), *Archaeological Chemistry: Analytical Techniques and Archaeological Interpretation* (pp. 460–479). Washington: American Chemical Society.

Killick, D. (2015). The awkward adolescence of archaeological science. *Journal of Archaeological Science, 56*, 242–247.

Kingery-Schwartz, A., Popelka-Filcoff, R. S., Lopez, D. A., Pottier, F., Hill, P., & Glascock, M. (2013). Analysis of geological ochre: its geochemistry, use, and exchange in the US Northern Great Plains. *Open Journal of Archaeometry, 1*, e15.

Klaproth, M. H. (1798). Mémoire de numismatique docimastique. *Mémoires de l'Academie Royale des Sciences et Belles-Lettres. Classe de Philosophie Expérimentale*, 97–113.

Korkmaz, S., Goksuluk, D., & Zararsiz, G. (2014). MVN: an R package for assessing multivariate normality. *The R Journal, 6*(2), 151–162.

Longerich, H. P., Jackson, S. E., & Günther, D. (1996). Laser ablation inductively coupled plasma mass spectrometric transient signal data acquisition and analyte concentration calculation. *Journal of Analytical Atomic Spectrometry, 11*, 899–904.

Lowe, D. J., Pearce, N. J., Jorgensen, M. A., Kuehn, S. C., Tryon, C. A., & Hayward, C. L. (2017). Correlating tephras and cryptotephras using glass compositional analyses and numerical and statistical methods: Review and evaluation. *Quaternary Science Reviews, 175*, 1–44.

MacDonald, B. L., Hancock, R. G. V., Cannon, A., McNeill, F., Reimer, R., & Pidruczny, A. (2013). Elemental analysis of ochre outcrops in southern British Columbia, Canada. *Archaeometry, 55*(6), 1020–1033.

MacDonald, B. L., Fox, W., Dubreuil, L., Beddard, J., & Pidruczny, A. (2018). Iron oxide geochemistry in the Great Lakes region (North America): Implications for ochre provenance studies. *Journal of Archaeological Science: Reports, 19*, 476–490.

Mackay, A., & Welz, A. (2008). Engraved ochre from a middle stone age context at Klein Kliphuis in the Western Cape of South Africa. *Journal of Archaeological Science, 35*, 1521–1532.

Mardia, K. V. (1970). Measures of multivariate skewness and kurtosis with applications. *Biometrika, 57*, 519–530.

Mardia, K. V. (1974). Applications of some measures of multivariate skewness and kurtosis for testing normality and robustness studies. *Sankhya, 36*, 115–128.

Martín-Fernández, J. A., Barceló-Vidal, C., & Pawlowsky-Glahn, V. (2000). Zero replacement in compositional data sets. In H. Kiers, J. Rasson, P. Groenen, & M. Shader (Eds.), *Data analysis, classification, and related methods* (pp. 155–160). Berlin: Springer-Verlag.

Martín-Fernández, J. A., Barceló-Vidal, C., & Pawlowsky-Glahn, V. (2003). Dealing with zeros and missing values in compositional data sets using nonparametric imputation. *Mathematical Geology, 35*, 253–278.

Mathis, F., Bodu, P., Dubreuil, O., & Salomon, H. (2014). PIXE identification of the provenance of ferruginous rocks used by Neanderthals. *Nuclear Instruments and Methods in Physics Research, Section B: Beam Interactions with Materials and Atoms, 331*, 275–279.

Mills, P. R., Lundblad, S. P., Smith, J. G., McCoy, P. C., & Naleimaile, S. P. (2008). Science and sensitivity: a geochemical characterization of the Mauna Kea adze quarry complex, Hawai'i Island, Hawaii. *American Antiquity, 73*(4), 743–758.

Ministry of Energy and Regional Development of Kenya (1987). Geological map of Kenya, scale 1:1,000,000. Nairobi.

Moens, L., & Dams, R. (1995). NAA and ICP-MS: a comparison between two methods for trace and ultra-trace element analysis. *Journal of Radioanalytical and Nuclear Chemistry, 192*, 29–38.

Moyo, S., Mphuthi, D., Cukrowska, E., Henshilwood, C. S., van Niekerk, K., & Chimuka, L. (2016). Blombos Cave: middle stone age ochre differentiation through FTIR, ICP OES, ED XRF and XRD. *Quaternary International, 404*(B), 20–29.

Nakamura, K. (2005). *Adornments of the Samburu in Northern Kenya: a comprehensive list*. Kyoto: Center for African Area Studies, Kyoto University.

Nakayama, K., Ichikawa, S., & Nakamura, T. (2012). Glass bead with minimized amount (11 mg) of sample for X-ray fluorescence determination of archaeological ceramics. *X-Ray Spectrometry, 41*(1), 16–21.

Neff, H. (2000). Neutron activation analysis for provenance determination in archaeology. In E. Ciliberto & G. Spoto (Eds.), *Modern Analytical Methods in Art and Archaeology. Chemical Analysis Series* (Vol. 155, pp. 81–133). New York: John Wiley, & Sons.

Nesbitt, R. W., Hirata, T., Butler, I. B., & Milton, J. A. (1997). UV laser ablation ICP-MS: some applications in the earth sciences. *Geostandards Newsletter: The Journal of Geostandards and Geoanalysis, 20*(2), 231–243.

Palarea-Albaladejo, J., & Martin-Fernandez, J. A. (2013). Values below detection limit in compositional chemical data. *Analytica Chimica Acta, 764*, 32–43.

Palarea-Albaladejo, J., Martín-Fernández, J. A., & Buccianti, A. (2014). Compositional methods for estimating elemental concentrations below the limit of detection in practice using R. *Journal of Geochemical Exploration, 141*, 71–77.

Paton, C., Hellstrom, J., Paul, B., Woodhead, J., & Hergt, J. (2011). Iolite: freeware for the visualisation and processing of mass spectrometric data. *Journal of Analytical Atomic Spectrometry, 26*, 2508–2518.

Pearson, G. (1796). Observations on some ancient metallic arms and utensils; with experiments to determine their composition. *Philosophical Transactions of the Royal Society of London, 86*, 395–451.

Pollard, A. M., & Heron, C. (2008). *Archaeological Chemistry* (2nd ed.). Cambridge: The Royal Society of Chemistry.

Pollard, A. M., Batt, C. M., Stern, B., & Young, S. M. M. (2007). *Analytical Chemistry in Archaeology*. Cambridge: Cambridge University Press.

Pollard, A. M., Bray, P. J., & Gosden, C. (2014). Is there something missing in scientific provenance studies of prehistoric artefacts? *Antiquity, 88*, 625–631.

Popelka-Filcoff, R. S. (2006). *Applications of elemental analysis for archaeometric studies: analytical and statistical methods for understanding geochemical trends in ceramics, ochre and obsidian*. Doctoral dissertation: University of Missouri-Columbia.

Popelka-Filcoff, R. S., Robertson, J. D., Glascock, M. D., & Descantes, C. (2007). Trace element characterization of ochre from geological sources. *Journal of Radioanalytical and Nuclear Chemistry, 272*, 17–27.

Popelka-Filcoff, R. S., Miksa, E. J., Robertson, J. D., Glascock, M. D., & Wallace, H. (2008). Elemental analysis and characterization of ochre sources from southern Arizona. *Journal of Archaeological Science, 35*, 752–762.

Popelka-Filcoff, R. S., Lenehan, C. E., Glascock, M. D., Bennett, J. W., Stopic, A., Quinton, J. S., Pring, A., & Walshe, K. (2012). Evaluation of relative comparator and k0-NAA for characterization of aboriginal Australian ochre. *Journal of Radioanalytical and Nuclear Chemistry, 291*(1), 19–24.

Prendergast, M. E., & Sawchuk, E. (2018). Boots on the ground in Africa's ancient DNA 'revolution': archaeological perspectives on ethics and best practices. *Antiquity, 92*(363), 803–815.

Price, T. D., & Burton, J. H. (2011). *An Introduction to Archaeological Chemistry*. New York: Springer Science & Business Media.

Renfrew, C. (1977). Alternative models for exchange and spatial distribution. In T. K. Earle & J. E. Ericson (Eds.), *Exchange Systems in Prehistory* (pp. 71–90). New York: Academic Press.

Rifkin, R. F. (2015). Ethnographic and experimental perspectives on the efficacy of ochre as a mosquito repellent. *The South African Archaeological Bulletin, 70*, 64–75.

Rifkin, R. F., Dayet, L., Queffelec, A., Summers, B., Lategan, M., & d'Errico, F. (2015). Evaluating the photoprotective effects of ochre on human skin by in vivo SPF assessment: implications for human evolution, adaptation and dispersal. *PLoS One, 10*, e0136090.

Royston, J. P. (1982). An extension of Shapiro and Wilk's W test for normality in large samples. *Applied Statistics, 31*, 115–124.

Royston, J. P. (1983). Some techniques for assessing multivariate normality based on the Shapiro–Wilk W. *Applied Statistics, 32*, 121–133.

Russ, J., Bu, K., Hamrick, J., & Cizdziel, J. V. (2012). Laser ablation-inductively coupled plasma-mass spectrometry analysis of lower Pecos rock paints and possible pigment sources. In P. L. Lang & R. A. Armitage (Eds.), *ACS Symposium Series Volume 1103: Collaborative Endeavors in the Chemical Analysis of Art and Cultural Heritage Materials* (pp. 91–121). Washington: American Chemical Society.

Saitoti, T. O. (1993). *Maasai*. New York: Abradale Press.

Sajó, I. E., Kovács, J., Fitzsimmons, K. E., Jáger, V., Lengyel, G., Viola, B., Talamo, S., & Hublin, J. J. (2015). Core-shell processing of natural pigment: Upper Palaeolithic red ochre from Lovas, Hungary. *PLoS One, 10*, e0131762.

Sanford, R. F., Pierson, C. T., & Crovelli, R. A. (1993). An objective replacement method for censored geochemical data. *Mathematical Geology, 25*, 59–80.

Scadding, R., Winton, V., & Brown, V. (2015). An LA-ICP-MS trace element classification of ochres in the Weld Range environ, Mid West region, Western Australia. *Journal of Archaeological Science, 54*, 300–312.

Scheid, N., Becker, S., Dücking, M., Hampel, G., Kratz, J. V., Watzke, P., Weis, P., & Zauner, S. (2009). Forensic investigation of brick stones using instrumental neutron activation analysis (INAA), laser ablation–inductively coupled plasma–mass spectrometry (LA–ICP–MS) and X-ray fluorescence analysis (XRF). *Applied Radiation and Isotopes, 67*(12), 2128–2132.

Skala, W. (1979). Some effects of the constant-sum problem in geochemistry. *Chemical Geology, 27*, 1–9.

Smith, M. A., Fankhauser, B., & Jercher, M. (1998). The changing provenance of red ochre at Puritjarra rock shelter, Central Australia: Late Pleistocene to present. *Proceedings of the Prehistoric Society, 64*, 275–292.

Sylvester, P. J., & Jackson, S. E. (2016). A brief history of laser ablation inductively coupled plasma mass spectrometry (LA–ICP–MS). *Elements, 12*, 307–310.

Thackeray, A. I., Thackeray, J. F., & Beaumont, P. B. (1983). Excavations at the Blinkklipkop specularite mine near Postmasburg, Northern Cape. *South African Archaeological Bulletin, 38*, 17–25.

Thío-Henestrosa, S., & Martín-Fernández, J. A. (2005). Dealing with compositional data: the freeware CoDaPack. *Mathematical Geology, 37*, 773–793.

Trinkaus, E., & Buzhilova, A. P. (2018). Diversity and differential disposal of the dead at Sunghir. *Antiquity, 92*(361), 7–21.

Velliky, E. C., Barbieri, A., Porr, M., Conard, N. J., & MacDonald, B. L. (2019). A preliminary study on ochre sources in Southwestern Germany and its potential for ochre provenance during the Upper Paleolithic. *Journal of Archaeological Science: Reports, 27*, 101977.

Wadley, L. (2005). Putting ochre to the test: replication studies of adhesives that may have been used for hafting tools in the middle stone age. *Journal of Human Evolution, 49*(5), 587–601.

Weigand, P. C., Harbottle, G., & Sayre, E. V. (1977). Turquoise sources and source analysis: Mesoamerican and the southwestern U.S.A. In T. K. Earle & J. E. Ericson (Eds.), *Exchange Systems in Prehistory* (pp. 15–34). New York: Academic Press.

Williamson, R. F., & Pfeiffer, S. (2003). *Bones of the ancestors: the archaeology and osteobiography of the Moatfield ossuary. Mercury Series, 163*. Gatineau: Canadian Museum of Civilization.

Wilson, L., & Pollard, A. M. (2001). The provenance hypothesis. In D. R. Brothwell & A. M. Pollard (Eds.), *Handbook of Archaeological Sciences* (pp. 507–517). Chichester: John Wiley, & Sons.

Wreschner, E. E., Bolton, R., Butzer, K. W., Delporte, H., Häusler, A., Heinrich, A., Jacobson-Widding, A., Malinowski, T., Masset, C., Miller, S. F., Ronen, A., Solecki, R., Stephenson, P. H., Thomas, L. L., & Zollinger, H. (1980). Red ochre and human evolution: a case for discussion [and comments and reply]. *Current Anthropology, 21*, 631–644.

Zhu, T., Sun, W., Zhang, H., Wang, H., Kuang, G., & Lv, L. (2012). Study on the provenance of Xicun Qingbai wares from the northern Song dynasty of China. *Archaeometry, 54*(3), 475–488.

Zipkin, A. M., Wagner, M., McGrath, K., Brooks, A. S., & Lucas, P. W. (2014). An experimental study of hafting adhesives and the implications for compound tool technology. *PLoS One, 9*, e112560.

Zipkin, A. M., Hanchar, J. M., Brooks, A. S., Grabowski, M. W., Thompson, J. C., & Gomani-Chindebvu, E. (2015). Ochre fingerprints: distinguishing among Malawian mineral pigment sources with homogenized ochre chip LA–ICPMS. *Archaeometry, 57*(2), 297–317.

Zipkin, A. M., Ambrose, S. H., Hanchar, J. M., Piccoli, P. M., Brooks, A. S., & Anthony, E. Y. (2017). Elemental fingerprinting of Kenya Rift Valley ochre deposits for provenance studies of rock art and archaeological pigments. *Quaternary International, 430*, 42–59.

Affiliations

Andrew M. Zipkin[1,2] · Stanley H. Ambrose[1] · Craig C. Lundstrom[3] · Gideon Bartov[3] · Alyssa Dwyer[4] · Alexander H. Taylor[3]

✉ Andrew M. Zipkin
andrew.zipkin@asu.edu

[1] Department of Anthropology, University of Illinois at Urbana-Champaign, 109 Davenport Hall, 607 S. Mathews Ave, Urbana, IL 61801, USA

[2] School of Human Evolution and Social Change, Arizona State University, P.O. Box 872402, Tempe, AZ 85287-2402, USA

[3] Department of Geology, University of Illinois at Urbana-Champaign, 3086 Natural History Building, 1301 West Green Street, Urbana, IL 61801, USA

[4] Department of Chemistry, University of Illinois at Urbana-Champaign, 505 S. Mathews Avenue, Urbana, IL 61801, USA